"Analysis and Implementation of a Bidirectional DC-DC Converter"

Major Project Report

Submitted in Partial Fulfillment of the Requirements for the Degree of

MASTER OF TECHNOLOGY

IN

ELECTRICAL ENGINEERING
(Power Electronics, Machines & Drives)

By

Honey R. Sharma
(12MEEP25)

Department of Electrical Engineering
INSTITUTE OF TECHNOLOGY
NIRMA UNIVERSITY
AHMEDABAD 382 481

May 2014

Undertaking for Originality of the Work

I **Honey R. Sharma**, Roll No. **12MEEP25**, give undertaking that the Major Project entitled **"Analysis and Implementation of a Bidirectional DC - DC Converter"** submitted by me, towards the partial fulfillment of the requirements for the degree of Master of Technology in **Power Electronics Machines** & **Drives, Electrical Engineering**, under Institute of Technology of Nirma University, Ahmedabad, is the original work carried out by me and I give assurance that no attempt of plagiarism has been made. I understand that in the event of any similarity found subsequently with any published work or any dissertation work elsewhere; it will result in severe disciplinary action.

.....

Signature of Student

Date:

Place:

Endorsed by:

.....

(Signature of Project Guide)

Prof. P. N. Kapil

Department of Electrical Engineering

Institute of Technology

Nirma University

Ahmedabad

CERTIFICATE

This is to certify that the Major Project Report entitled **"Analysis and Implementation of a Bidirectional DC-DC Converter"** submitted by **Ms. Honey R. Sharma** (**Roll No.: 12MEEP25**) towards the partial fulfillment of the requirements for Master of Technology (Electrical Engineering) in the field of Power Electronics, Machines & Drives of Nirma University, is the record of work carried out by her under our supervision and guidance. The work submitted has in our opinion reached a level required for being accepted for examination. The results embodied in this major project work to the best of our knowledge have not been submitted to any other University or Institution for award of any degree or diploma.

Date:

.....

Institute Guide

Prof. P.N. Kapil

Department of Electrical Engineering

Institute of Technology

Nirma University

Ahmedabad.

.....

Head of Department

Department of Electrical Engineering

Institute of Technology

Nirma University

Ahmedabad.

.....

Director

Institute of Technology

Nirma University

Ahmedabad.

Acknowledgement

I take this opportunity with much pleasure to thank all the people who have helped me throughout my project work. I wish to express my profound thanks to all those persons who co-operated with me converting my thoughts into a reality.

I feel privileged and would like to express my deepest gratitude to my Respected Internal Guide, Prof. P.N. Kapil, Assistant Professor, at Department of Electrical Engineering, Institute of Technology, Nirma University, Ahmedabad, who gave me the challenging task, trusted me to fulfill that task, gave his valuable suggestions, helping me constantly all through the way.

I am also indebted to Dr. P.N. Tekwani, Head of the Department, for his moral support and for all the problem solutions throughout project work.

I also express my sincere thanks to all the faculty members and supporting staff of the department for their invaluable support during the project duration. I would also like to thank Dr. K. Kotecha, the Director of Institute of Technology, Nirma University for providing the infrastructure to carry out the project work in the campus.

I am also very lucky to have such friends who co-operated me in the laboratory sessions and family too who were always there when needed the most.

Lastly I would like to thank Almighty, without whom all of us are nothing.

Honey R. Sharma

12MEEP25

Abstract

Here a bidirectional DC-DC converter has been presented and analysed. Bidirectional DC-DC converters are used for transferring the power, between any two DC sources in any forward or reverse direction. These type of converters are widely used in applications like HEV energy systems, fuel-cell hybrid power systems, UPS systems, Photo-voltaic hybrid power systems, and battery chargers. Different topologies of bidirectional dc-dc converters are studied for reference. The configuration of the adopted BDC is very easy to understand.

In the adopted converter, a coupled inductor has been employed with same no. of winding turns at the primary and secondary sides. The design of the coupled inductor is done selecting the appropriate parameters of the core and the conductor. The hardware includes the driver circuit for Mosfet, power supply for it, power circuit and testing the results in the open loop system, by giving the pwm control pulses through the Arduino Uno R3 controller. The adopted converter has higher step-up and step-down voltage gains than the conventional bidirectional DC-DC boost/buck converter. The study of operating principle and steady-state analysis is done. The project work includes the study, design, open loop and closed loop simulation, analysis of the adopted converter, and finally implementation of the development of the system integration and testing the experimental results.

List of Figures

2.1 Battery charger/discharger circuit 5
2.2 Solar cell PV energy system 6
2.3 A coupled inductor 8

3.1 Adopted bidirectional DC-DC converter 11
3.2 Adopted converter in step-up mode 11
3.3 Current flow path in step-up mode: Mode 1 12
3.4 Current flow path in step-up mode: Mode 2 13
3.5 Adopted converter in step-down mode 14
3.6 Current flow path in step-down mode: Mode 1 15
3.7 Current flow path in step-down mode: Mode 2 16

4.1 Model in step-up mode 18
4.2 Waveforms in step-up mode-part I 19
4.3 Waveforms in step-up mode-part II 20
4.4 Waveforms in step-down mode-part I 21
4.5 Waveforms in step-down mode- part II 22

5.1 Block diagram for closed loop system 23
5.2 Closed loop waveforms in step-up mode- part I 25
5.3 Closed loop waveforms in step-up mode-part II 26
5.4 Closed loop waveforms in step-down mode-part I 27
5.5 Closed loop waveforms in step-down mode-part II 28
5.6 Waveforms in step-up mode for overload condition 30
5.7 Waveforms in step-down mode for overload condition 31

6.1 Designed coupled inductor 36
6.2 Designed coupled inductor at 20 kHz 38

7.1 Waveforms at 20 kHz in step-up mode-part I 40
7.2 Waveforms at 20 kHz in step-up mode-part II 41
7.3 Waveforms at 20 kHz in step-down mode-part I 42
7.4 Waveforms at 20 kHz in step-down mode-part II 43

8.1 Driver circuit using TLP250 46
8.2 High and low Gate pulses for Mosfet 47
8.3 Power supply circuit for gate driver 47
8.4 Gate Driver Card 48

9.1 Front view of Arduino Uno 50
9.2 PWM Technique in Controller 51
9.3 Control pulse at 20kHz 52

10.1 The Converter system set-up 53
10.2 Power circuit set-up 54

Abbreviations

BDC ..... Bidirectional DC-DC Converter
MOSFET ..... Metal Oxide Field Effect Transistor
PWM ..... Pulse Width Modulation
UPS ..... Uninterrupted Power Supply
PV ..... Photo Voltaic
HEV ..... Hybrid Electric Vehicle
CCM ..... Continuous Conduction Mode
DCM ..... Discontinuous Conduction Mode
GaAlAs ..... Gallium Aluminum Arsenide
ESR ..... Equivalent series resistance
AP ..... Area Product
MLT ..... Mean length per turn
SWG ..... Standard wire gauge

Nomenclature

V_L ..... Low side Voltage

V_H ..... High side Voltage

k ..... Coupling coefficient of inductor

L_1 ..... Inductance of primary winding

L_2 ..... Inductance of secondary winding

V_{L1} ..... Voltage across primary winding

V_{L2} ..... Voltage across secondary winding

D ..... Duty ratio

r_{L1} ..... ESR of primary winding

r_{L2} ..... ESR of secondary winding

f_s ..... Switching frequency.

V_{DSS} ..... Maximum drain-source voltage

$R_{DS(ON)}$ ..... On state resistance

I_D ..... Max peak drain current

r_{S1} ..... On state resistance of switch S1

r_{S2} ..... On state resistance of switch S2

r_{S3} ..... On state resistance of switch S3

P_o ..... Output Power

I_{FL} ..... Output full load current

I_{pk} ..... Max peak value of inductor current

I_{rms} ..... Rms value of inductor current

B_{max} ..... Max flux density for ferrite core

K_w ..... Core window utilization factor

A_e ..... Magnetic core cross section area

A_w ..... Winding window area

N_{min} ..... Minimum no. of turns

l_{gap} ..... Air gap length

a .... cross section area of wire

J .... Current density

Contents

Undertaking ii

Certificate iii

Acknowledgement iv

Abstract v

List of Figures vi

Abbreviations/Nomenclature viii

Contents xi

1 Introduction 1
- 1.1 Project Objective . . . 1
- 1.2 Problem Identification . . . 2
- 1.3 Solution to the problem . . . 2
- 1.4 Scope of the work . . . 3

2 Review of DC-DC Converters 4
- 2.1 Applications of BDC . . . 4
  - 2.1.1 Application in battery charger circuits . . . 4
  - 2.1.2 Application in PV energy systems . . . 6
  - 2.1.3 Application in HEV systems . . . 6
- 2.2 Classification of dc- dc converters . . . 7
- 2.3 DC-DC Converter with coupled inductor . . . 8

3 Description of Adopted Topology 10
- 3.1 Adopted bidirectional dc-dc converter . . . 10
- 3.2 Step-up mode of Adopted Converter . . . 11
  - 3.2.1 Mode 1 . . . 12
  - 3.2.2 Mode 2 . . . 13
- 3.3 Step-down mode of Adopted Converter . . . 14

3.3.1 Mode 1 . . . 15
3.3.2 Mode 2 . . . 15

4 Simulation for open loop system 17
4.1 Step-up Operation . . . 17
4.2 Step-down Operation . . . 21

5 Simulation for closed loop system 23
5.1 Step-up Operation . . . 24
5.2 Step-down Operation . . . 27
5.3 Simulation for dynamic condition . . . 29

6 Design of the Coupled Inductor 32
6.1 Design Procedure for $f_s = 50kHz$ and $L = 35\mu H$ . . . 33
6.1.1 Selection of the Proper Core Size . . . 33
6.1.2 Calculation of no. of turns . . . 34
6.1.3 Selection of wire gauge . . . 35
6.2 Design Procedure for $f_s = 20kHz$ and $L = 140\mu H$ . . . 36

7 Simulation at reduced frequency 39
7.1 Step-up Operation . . . 39
7.2 Step-down Operation . . . 42

8 Driver circuit Implementation 44
8.1 Driver Circuit using TLP250 . . . 44
8.2 Power Supply for the driver circuit . . . 46

9 Programming through Controller 49
9.1 Introduction to Arduino . . . 49
9.1.1 Arduino Uno R3 . . . 49
9.2 Programming Description . . . 50

10 Testing the Hardware Set-up 53
10.1 Power Circuit . . . 54
10.2 Observation Results . . . 55

11 Conclusion and Future Work 56
11.1 Conclusion . . . 56
11.2 Future Work . . . 56

References 58

A Ferrite core properties 60

B SWG Table 62

Chapter 1

Introduction

1.1 Project Objective

The world is now habituated with the electronics devices without which it is very difficult for the mankind to keep going. So it is very important to develop the devices error free and fast response with high efficiency. Of the research field is dc-dc converters. The dc-dc converters mean the input is dc and the output is also dc. The two basic dc-dc converters are buck converter and boost converter. Based on these two converters, all other converters are derived. These converters can be classified based on various categories. The aim of developing the converters are high efficiency and high gain with fast response.

One such type of converter is bidirectional buck-boost converter. In this type of converter, one direction is used to step-up the voltage and another direction is used to step-down the voltage. It is just like the charging and discharging of the converter. Thus bidirectional DC-DC converters are used to transfer the power between two DC sources in either direction. These converters are widely used in applications, such as hybrid electric vehicle energy systems, uninterrupted power supplies, fuel-cell hybrid power systems, PV hybrid power systems, and battery chargers.

1.2 Problem Identification

Todays world demands the low power application devices which is the focus of the researchers. There are so many parameters involved while developing the converters. Applications that require exchange of power from the source to the load and vice versa have conventionally been implemented with two uni-directional converters, each processing the power in one direction[1]. With growing emphasis on compact, smaller and efficient power systems, there is increasing interest in the possibility of using bidirectional converters, especially in DC power based applications like space, telecommunication and computer systems. The escalating cost of energy in recent years has resulted in growing emphasis on energy management due to the drain on natural resources and environmental pollution, and energy saving techniques are becoming more important. The demand for the development of sophisticated, compact and efficient power systems has prompted research in bi-directional converters providing the desired bilateral power flow and capable of replacing the two unidirectional converters.

1.3 Solution to the problem

A bi-directional dc-dc converter, capable of bilateral power flow, provides the functionality of two uni directional converters in a single converter unit. The focus of bidirectional dc-dc converter topologies has been primarily on medium and high power applications with few topologies presented for low power applications. The high power dc-dc converters use either resonant, soft switching achieved by controlled phase shift or hard switched PWM. In general, despite their individual advantages, these topologies are unsuitable for low power applications due to one or all of the

following reasons:

Large number of switches,

High component count,

Many switches are active at any given instant of time and the gating pattern may be complicated,

Limited range of satisfactory operation with high efficiency,

Complex power and control circuitry.

So this project work presents a bi-directional dc-dc converter for low power applications like DC UPS systems, battery chargers, etc.

1.4 Scope of the work

The projects implements a bidirectional dc-dc converter using a coupled inductor. This type of converter must have higher step-up and step-down voltage gains and high efficiency too. The converter is simulated in the open loop as well as in the closed loop mode. The analysis of the results is done under the steady state and dynamic conditions like overload. The ratings/specifications of the components would be chosen according to the requirements of the converter used in applications like Automobile dual battery systems, UPS systems and battery chargers. Thus the requirements for the hardware implementation of the development of the system integration would be fulfilled.

Chapter 2

Review of DC-DC Converters

In this section, previous work in the area of bi-directional dc-dc converters is reviewed with the objective of defining the current status of research in this area and evaluating topologies for their possible implementation in low power bi-directional dc-dc converters. Also some of the applications are discussed.

2.1 Applications of BDC

Bidirectional DC - DC converters play an important role in applications where conversion of DC to DC is involved. These applications include hybrid electric vehicles, switching mode power supplies, battery chargers, PV hybrid power systems and uninterruptible power supplies.

2.1.1 Application in battery charger circuits

A battery charger/discharger circuit is shown in the figure 2.1 where such a bidirectional converter can be implemented. The battery charger/ discharger circuit can be used as part of a DC UPS system. Conventional battery charger/discharger circuits

comprised of two converters; one for the charging the battery from a DC bus and the other to provide power to the DC bus from the battery. The adopted bi-directional converter provides both functions of battery charging and discharging in a single conversion unit with its bidirectional power flow capability[1]

To realize the double sided power flow in bidirectional dc-dc converters, the switch cell should carry the current on both directions. It is usually implemented with a unidirectional semiconductor power switch such as power MOSFET or IGBT in parallel with a diode, because the double sided current flow power switch is not available. For the buck and boost dc-dc type converters, the bidirectional power flow is realized by replacing the switch and diode with the double sided current switch cell.

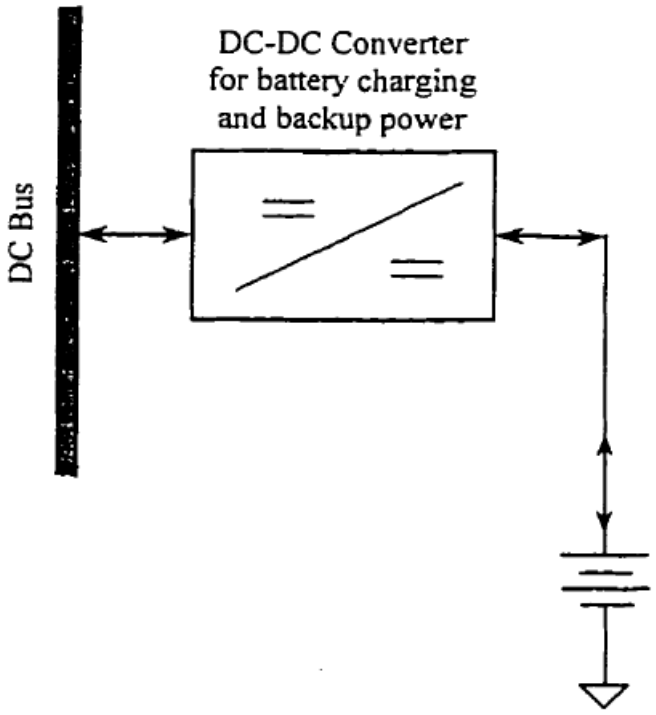

Figure 2.1: Battery charger/discharger circuit

2.1.2 Application in PV energy systems

Using clean energy resources like photovoltaic arrays and wind turbines in renewable electric power generation systems, the bidirectional dc-dc converter is used to transfer the solar energy to the capacitive energy source during the sunny time, while to deliver energy to the load when the dc bus voltage is low. A PV power system with bidirectional converter is shown in figure 2.2 The bidirectional dc-dc converter is regulated by the solar array photovoltaic level, thus to maintain a stable load bus voltage and make fully usage of the solar array and the storage battery.

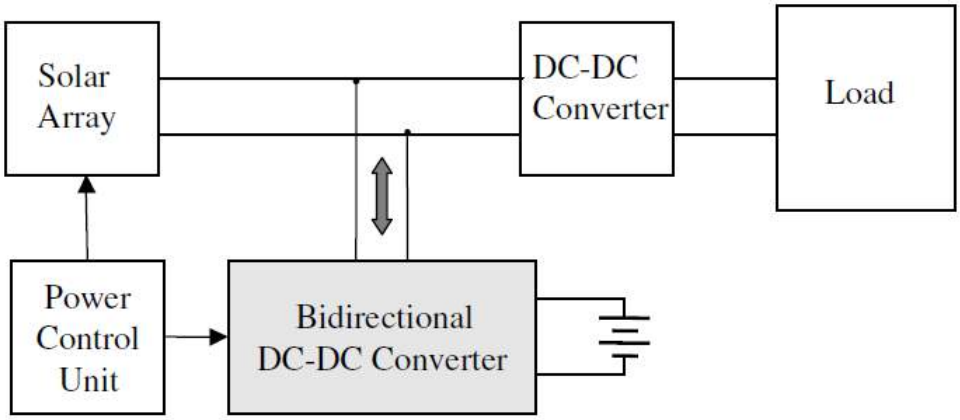

Figure 2.2: Solar cell PV energy system

2.1.3 Application in HEV systems

In the electric vehicle applications also, an auxiliary energy storage battery absorbs the regenerated energy fed back by the electric machine. So a bidirectional dc-dc converter is required to draw power from the auxiliary battery to boost the high-voltage bus during vehicle starting, acceleration and hill climbing.[15]

2.2 Classification of dc- dc converters

DC-DC converters can be classified based on various categories. These converters can be classified as isolated and non-isolated converters, unidirectional and bidirectional converters, step-up and step-down converters, single input and multi-input converters, Low power application and high power application converters etc[2].

We can classify bidirectional dc-dc converters as isolated and non-isolated dc-dc converters. The isolated bidirectional dc-dc converters, include the half-bridge types and full-bridge types. These converters can provide high step-up and step-down voltage gain by adjusting the turns ratio of the transformer. But these mechanisms with isolated transformers have high conduction losses because four to nine power switches are required. Also the switching losses are increased.

For non-isolated applications, the non-isolated bidirectional DC-DC converters include the conventional boost/buck type, multi-level type, three-level type, sepic/zeta type, switched-capacitor type, and coupled-inductor type[3]. The multi-level type is a magnetic-less converter, but 12 switches are used in this converter. If higher step-up and step-down voltage gains are required, more switches are needed. Thus control circuit becomes more complicated. In the three-level type, the voltage stress across the switches on the three-level type is only half of the conventional type. However, the step-up and step-down voltage gains are low. Since the sepic/zeta type is combined of two power stages, the conversion efficiency will be decreased. The switched capacitor and coupled-inductor types can provide high step-up and step-down voltage gains. However in switched capacitor type, increased switching loss and current stress are the critical drawbacks.

2.3 DC-DC Converter with coupled inductor

The primary challenge is to design a circuit that has few switching devices and capacitors. So, a bidirectional dc-dc converter using a coupled inductor is implemented here consisting of three switches. The brief description the converter circuit is given in the next chapter.

The coupled inductor is the main energy transfer element in this converter. In each switching cycle it is charged through source side active switches for the duration of Ton=DT, where T=1/fsw is the switching period and D is the duty cycle. This energy is then discharged to load during Toff=(1-D)T.

A coupled inductor is the inductor with same winding turns in the primary and secondary sides as shown in fig 2.1

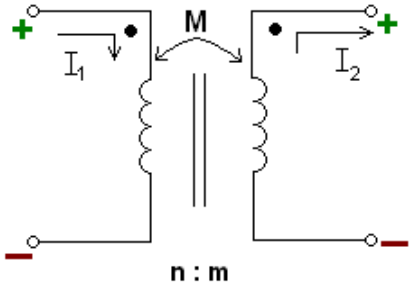

Figure 2.3: A coupled inductor

The pair of coupled coils shown in figure has currents, voltages and polarity dots indicated and $M_{12} = M_{21} = M$ where M is the mutual inductance. The degree to which M approaches its maximum value is described by the coupling coefficient k, defined as

$K = \frac{M}{\sqrt{L_1 L_2}}$

Since $M \leq \sqrt{L_1 L_2}$, $\quad 0 \leq k \leq 1$

The larger values of the coefficient of coupling are obtained with coils which are physically closer, which are wound or oriented to provide a larger common magnetic

flux, or provided with a common path through a material which serves to concentrate and localize the magnetic flux. Coils having a coefficient of coupling close to unity are said to be tightly coupled.

The factor k, the coupling coefficient represents the flux linkage between the two windings. Permissible values of k are 0 to 1. A value of 1 means that all the flux linking coil 1, also links coil 2. In practice, values of $k > 0.9$ are easily achievable. Since the coupling coefficient depends on geometry, changes in wire spacing or inconsistent winding techniques can cause variations from sample to sample.

Chapter 3

Description of Adopted Topology

The objective of this chapter is to describe in detail the topology, modes of operation and the control principle of the adopted bi-directional dc-dc converter . The basic elements of the converter, and their functionality are described in this section.
In the converter, the semiconductor devices are used as switching devices due to which the converters can operate at high frequencies. The different arrangement of inductors and capacitors in the converters operates as a filter circuit. The resistance act as a load in the circuit which can be varied to study the behaviour during light load and heavy load. The different types of input dc sources which are used are like battery, renewable energy sources etc.

3.1 Adopted bidirectional dc-dc converter

Here a novel bidirectional DC-DC converter is adopted, as shown in figure 3.1. The adopted converter employs a coupled inductor with same winding turns in the primary and secondary sides. The power MOSFETs S_1, S_2, S_3 are the primary switching devices of the adopted converter. They are gated at a constant frequency with variable on time to provide the necessary regulated output voltage.

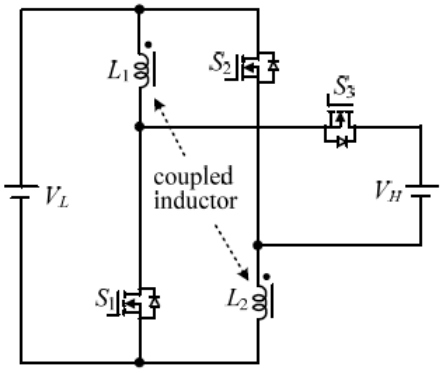

Figure 3.1: Adopted bidirectional DC-DC converter

The pulse-width modulation (PWM) technique is used to control the switches here.

3.2 Step-up mode of Adopted Converter

The adopted converter in step-up mode is shown in Fig. 3.2. The pulse-width modulation (PWM) technique is used to control the switches S_1 and S_2 simultaneously. The switch S_3 is the synchronous rectifier[6]. Since the primary and secondary wind-

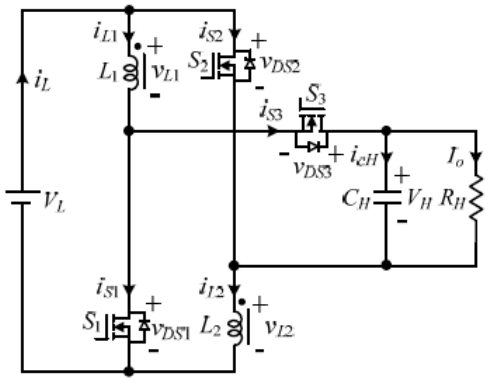

Figure 3.2: Adopted converter in step-up mode

ing turns of the coupled inductor is same, the inductance of the coupled inductor in the primary and secondary sides are expressed as

$$L_1 = L_2 = L \tag{3.1}$$

Thus, the mutual inductance M of the coupled inductor is given by

$$M = k\sqrt{L_1 L_2} = kL \tag{3.2}$$

where k is the coupling coefficient of the coupled inductor. The voltages across the primary and secondary windings of the coupled inductor are as follows:

$$V_{L1} = L_1 \frac{di_{L1}}{dt} + M\frac{di_{L2}}{dt} = L\frac{di_{L1}}{dt} + kL\frac{di_{L2}}{dt} \tag{3.3}$$

$$V_{L2} = M\frac{di_{L1}}{dt} + L_2\frac{di_{L2}}{dt} = kL\frac{di_{L1}}{dt} + L\frac{di_{L2}}{dt} \tag{3.4}$$

The operating principle and steady-state analysis of the converter in Continuous Conduction Mode (CCM) of operation is described as follows:

3.2.1 Mode 1

During this time interval $[t_0, t_1]$, S_1 and S_2 are turned on and S_3 is turned off. The current flow path is shown in fig 3.3. The energy of the low-voltage side V_L is trans-

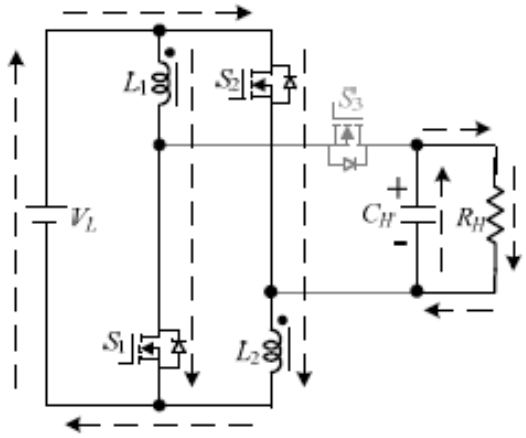

Figure 3.3: Current flow path in step-up mode: Mode 1

ferred to the coupled inductor. Meanwhile, the primary and secondary windings of the

coupled inductor are in parallel. The energy stored in the capacitor C_H is discharged to the load. Thus, the voltages across L_1 and L_2 are obtained as

$$v_{L1} = v_{L2} = V_L \tag{3.5}$$

Substituting (3.3) and (3.4) into (3.5), yielding

$$\frac{di_{L1}(t)}{dt} = \frac{di_{L2}(t)}{dt} = \frac{V_L}{(1+k)L}, \quad t_0 \leq t \leq t_1 \tag{3.6}$$

3.2.2 Mode 2

During this time interval $[t_1, t_2]$, S_1 and S_2 are turned off and S_3 is turned on. The current flow path is shown in fig.3.4. The low-voltage side V_L and the coupled inductor

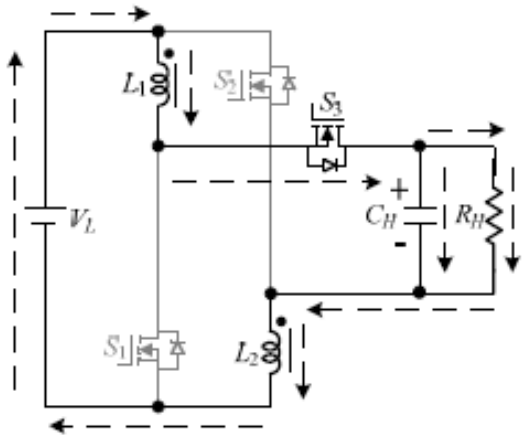

Figure 3.4: Current flow path in step-up mode: Mode 2

are in series to transfer their energies to the capacitor C_H and the load. Meanwhile, the primary and secondary windings of the coupled inductor are in series. Thus, the following equations are found to be

$$i_{L1} = i_{L2} \tag{3.7}$$

$$v_{L1} + v_{L2} = V_L - V_H \tag{3.8}$$

Substituting (3.3), (3.4), and (3.7) into (3.8), yielding

$$\frac{di_{L1}(t)}{dt} = \frac{di_{L2}(t)}{dt} = \frac{V_L - V_H}{2(1+k)L}, \quad t_1 \le t \le t_2 \tag{3.9}$$

By using the state-space averaging method, the following equation is derived from (3.6) and (3.9):

$$\frac{DV_L}{(1+k)L} + \frac{(1-D)(V_L - V_H)}{2(1+k)L} = 0 \tag{3.10}$$

Simplifying (3.10), the voltage gain is given as

$$G_{CCM(step-up)} = \frac{V_H}{V_L} = \frac{1+D}{1-D} \tag{3.11}$$

3.3 Step-down mode of Adopted Converter

Fig. 3.5 shows the adopted converter in step-down mode. The PWM technique is used to control the switch S_3. The switches S_1 and S_2 are the synchronous rectifiers. The

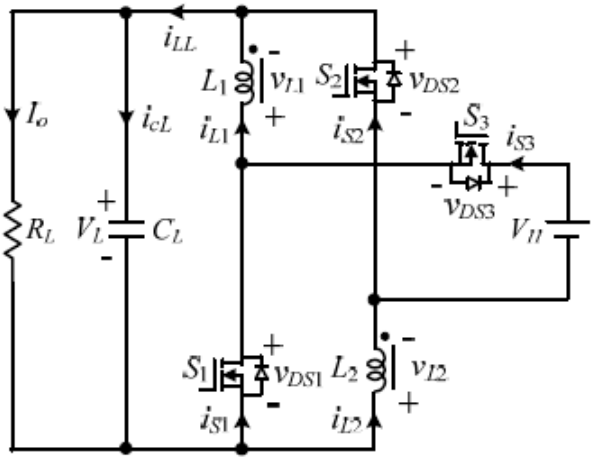

Figure 3.5: Adopted converter in step-down mode

operating principle and steady-state analysis in CCM mode of operation is described as follows:

3.3.1 Mode 1

During this time interval $[t_0, t_1]$, S_3 is turned on and S_1/S_2 are turned off. The current flow path is shown in Fig.3.6. The energy of the high-voltage side V_H is transferred

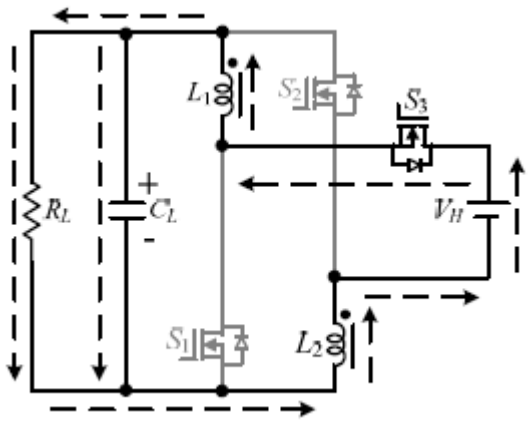

Figure 3.6: Current flow path in step-down mode: Mode 1

to the coupled inductor, the capacitor C_L, and the load. Meanwhile, the primary and secondary windings of the coupled inductor are in series. Thus, the following equations are given as

$$i_{L1} = i_{L2} \tag{3.12}$$

$$v_{L1} + v_{L2} = V_H - V_L \tag{3.13}$$

Substituting (3.3), (3.4), and (3.12) into (3.13), yielding

$$\frac{di_{L1}(t)}{dt} = \frac{di_{L2}(t)}{dt} = \frac{V_H - V_L}{2(1+k)L}, \quad t_0 \le t \le t_1 \tag{3.14}$$

3.3.2 Mode 2

During this time interval $[t_1, t_2]$, S_3 is turned off and S_1/S_2 are turned on. The current flow path is shown in Fig.3.7. The energy stored in the coupled inductor is released to the capacitor C_L and the load. Meanwhile, the primary and secondary windings of

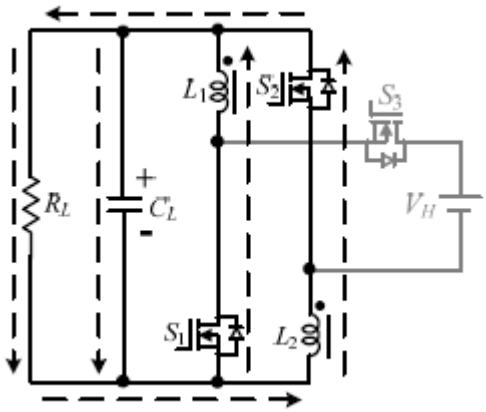

Figure 3.7: Current flow path in step-down mode: Mode 2

the coupled inductor are in parallel. Thus, the voltages across L_1 and L_2 are derived as

$$v_{L1} = v_{L2} = -V_L \tag{3.15}$$

Substituting (3.3) and (3.4) into (3.15), yielding

$$\frac{di_{L1}(t)}{dt} = \frac{di_{L2}(t)}{dt} = -\frac{V_L}{(1+k)L}, \quad t_1 \leq t \leq t_2 \tag{3.16}$$

By using the state-space averaging method, the following equation is obtained from (3.14) and (3.16):

$$\frac{D(V_H - V_L)}{2(1+k)L} - \frac{(1-D)V_L}{(1+k)L} = 0 \tag{3.17}$$

Simplifying (3.17), the voltage gain is found to be

$$G_{CCM(step-down)} = \frac{V_L}{V_H} = \frac{D}{2-D} \tag{3.18}$$

Chapter 4

Simulation for open loop system

The software meant for the Power Electronics Simulation, play a vital role in the design and analysis of the converters. Various types of software are used to simulate the converters in the initial level. Different types of software are MATLAB, PSIM, PSPICE, SABER, and MULTISIM. There are also different simulations approaches are used for detailed studies such as device level simulation, circuit level simulation and system level simulation. Different analysis are available in different simulators. Here the Simulation of the power circuit is carried out in PSIM 9.0.

4.1 Step-up Operation

The figure 4.1 given below shows the power circuit model of the adopted bidirectional dc dc converter in the step-up mode of operation. Here the circuit parameters are designed and selected as per the use of this converter in applications like Automobile dual battery systems, battery chargers, etc.

Here a 14/42-V converter circuit is simulated in the PSIM software for the automobile dual-battery system.

The electric specifications and circuit components are selected as $V_L = 14$ V, $V_H =$

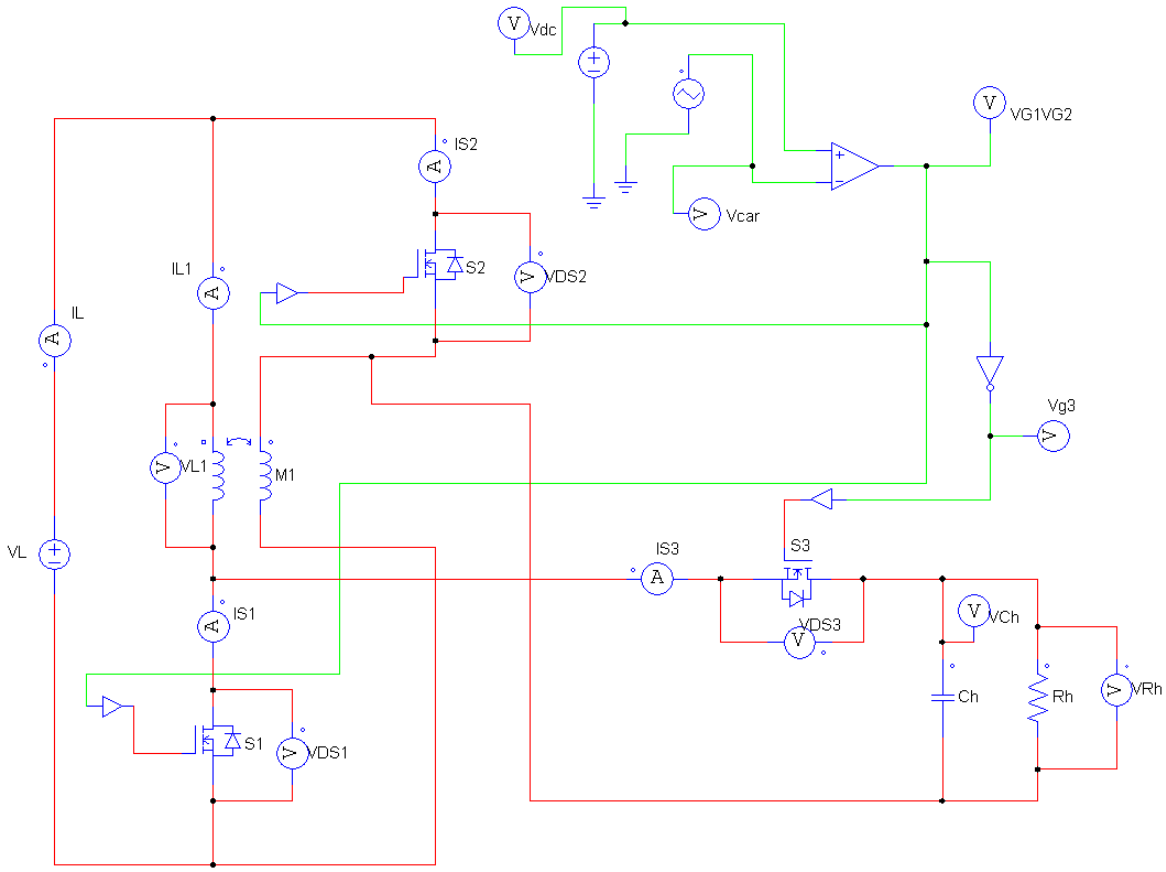

Figure 4.1: Model in step-up mode

42 V, fs = 50 kHz, Po = 200 W, $C_L = C_H = 330\mu F$, $L_1 = L_2 = 35\mu H$ ($r_{L1} = r_{L2} = 11m\Omega$ which represents the ESR of the inductance). $R_H = R_L = \frac{V_H^2}{Po} = 8.82\Omega$. Also, MOSFET IRF3710 ($V_{DSS} = 100V, R_{DS(ON)} = 23m\Omega, and I_D = 57A$) is selected for S_1, S_2, and S_3. Internal diode forward voltage = 1.2 V and internal diode resistance $R_d = \frac{1.2}{57} = 0.02\Omega$.

The PWM pulses are generated by comparing a reference dc signal with the carrier triangular signal having 50kHz frequency and then given to the gate of the Mosfet. Fig 4.2 and fig 4.3 shows the some of the simulated waveforms of the adopted converter in step-up mode for CCM mode of operation.

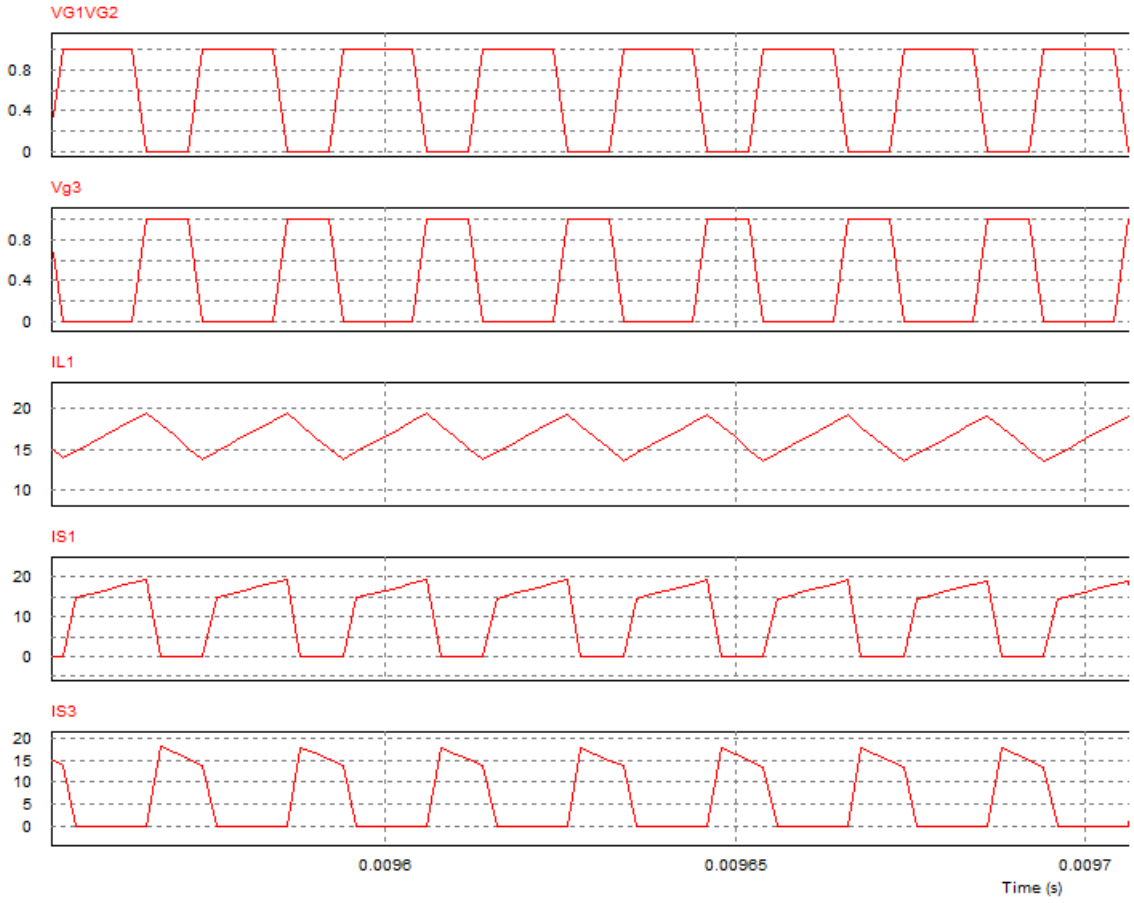

Figure 4.2: Waveforms in step-up mode-part I

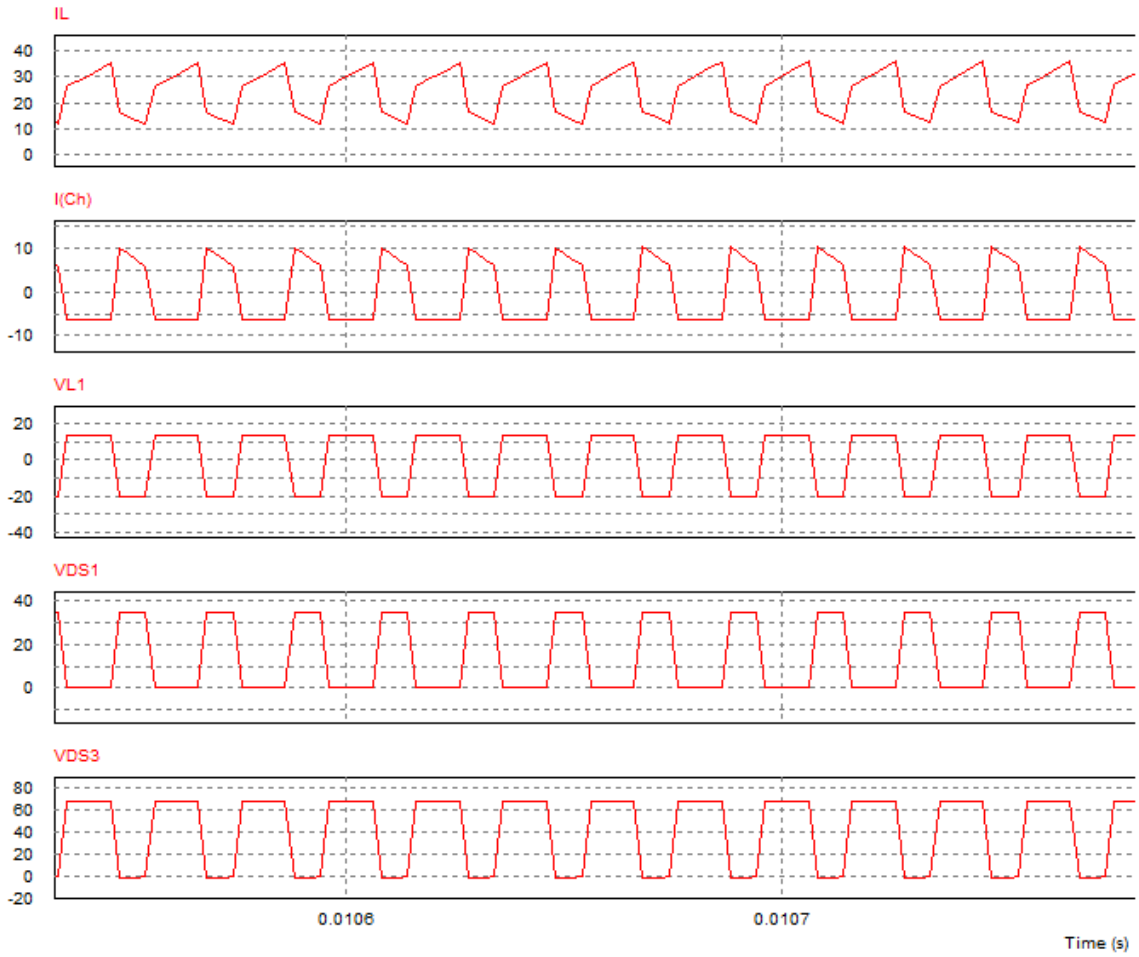

Figure 4.3: Waveforms in step-up mode-part II

4.2 Step-down Operation

The circuit parameters and specifications are kept same as that in the step-up mode of operation. Fig 4.4 and fig 4.5 shows the some of the simulated waveforms of the adopted converter in step-down mode for CCM mode of operation.

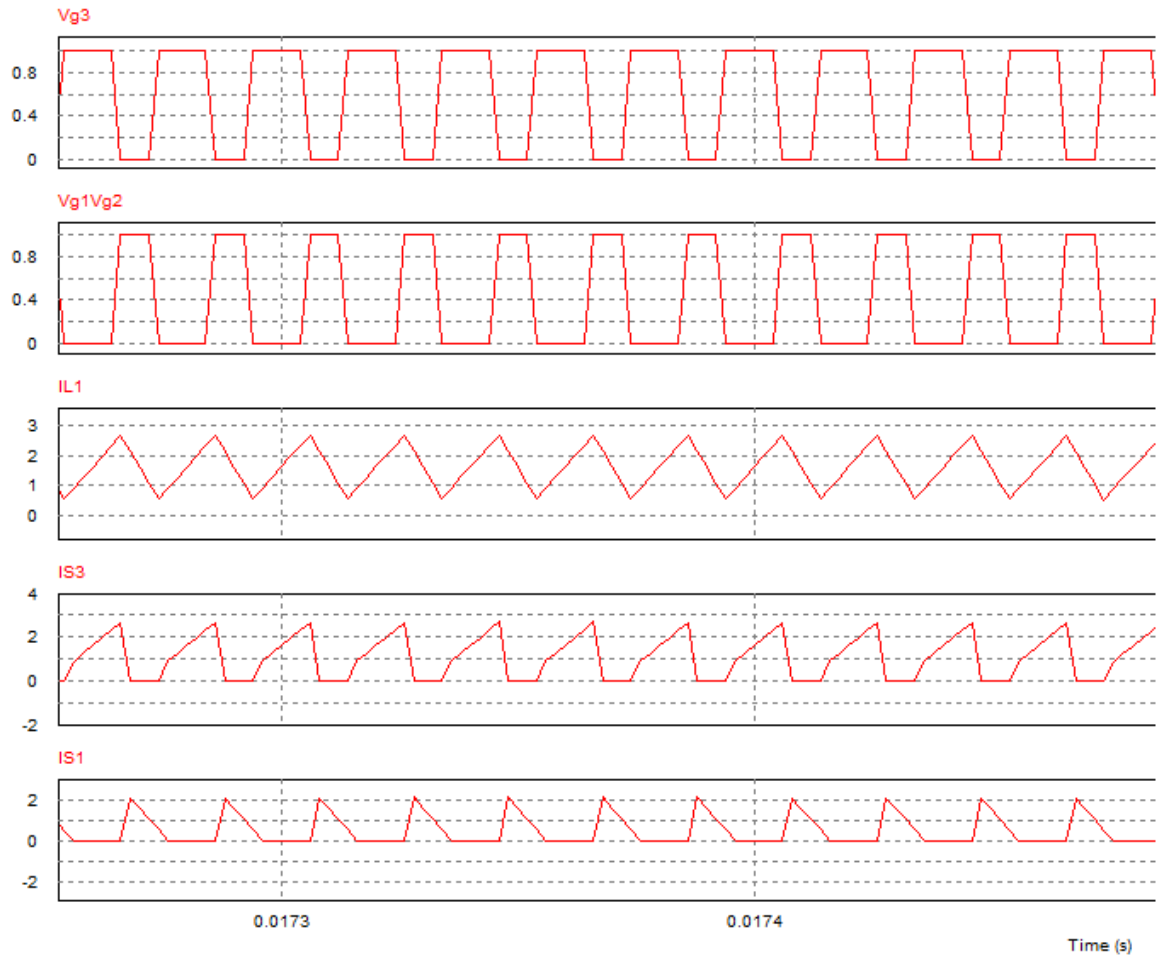

Figure 4.4: Waveforms in step-down mode-part I

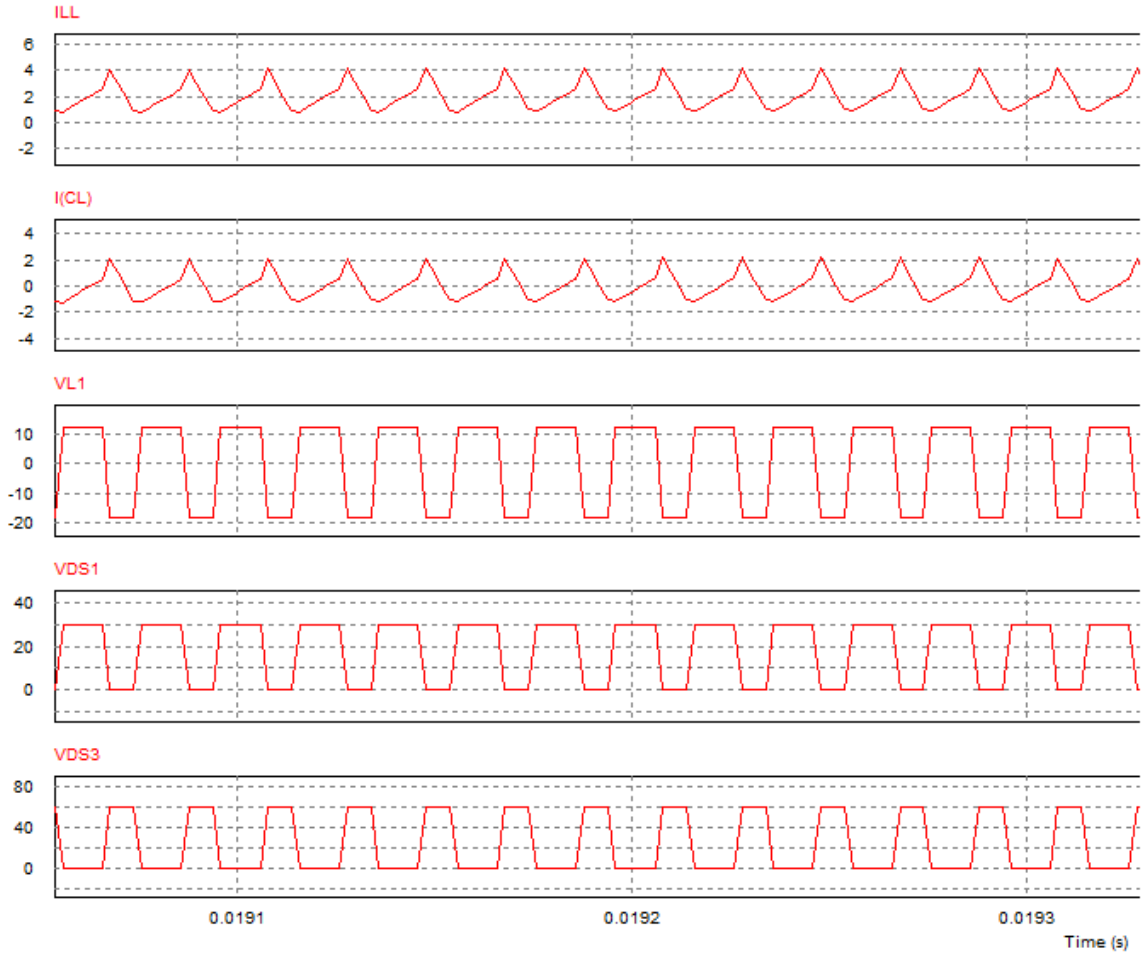

Figure 4.5: Waveforms in step-down mode- part II

Chapter 5

Simulation for closed loop system

Here in the closed loop system, a feedback loop is implemented from the load side. The general block diagram of the closed loop system is shown in fig 4.6.

The input dc source is either stepped up or stepped down to an another dc voltage,

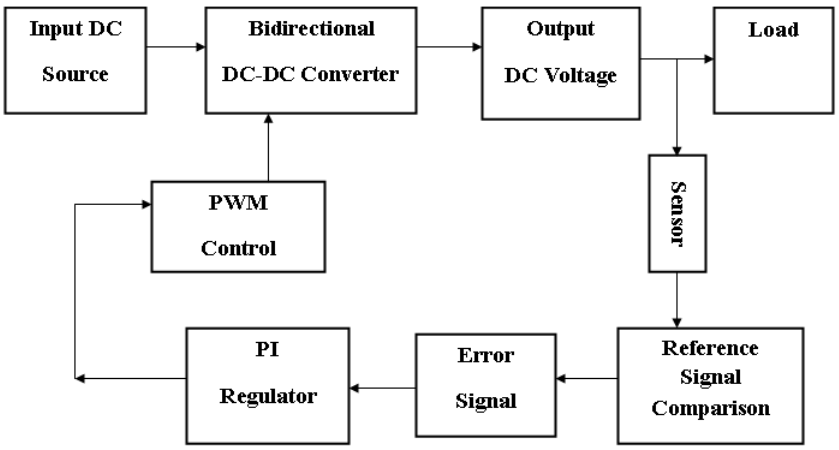

Figure 5.1: Block diagram for closed loop system

through the bidirectional dc-dc converter and given to the load. The output dc voltage is sensed through the voltage sensor and compared with the reference signal. The error signal is then sent to the PI controller.

A PI Controller is the combination of a Proportional and Integrative control. The

use of PI controller is very often in practical systems. A PI controller will eliminate forced oscillations resulting in operation of on-off controller. However, introducing integral mode has a negative effect on speed of the response and overall stability of the system[9]. Thus, PI controller will not increase the speed of response. They are very often used in industry, especially when speed of the response is not an issue and large disturbances and noise are present during operation of the process. The overall accuracy of the system improves.

In the software implementation of a PI Controller, gain and time constant are to be tuned. Tuning is adjustment of control parameters to the optimum values for the desired control response. Stability is a basic requirement. There are accordingly various methods for PI loop tuning. One of them is Manual Tuning method. In manual tuning method, parameters are adjusted by watching system responses. The value of the gain is changed until desired or required system response is obtained. This method is simple to implement. Here in the simulation, the gain is taken as 0.7 and time constant is taken as 0.008.

The output of the PI regulator is given to the PWM logic circuit from where controlled pulses are generated and given to the gate of the Mosfets.

5.1 Step-up Operation

The circuit parameters and specifications are kept same as that in the open loop system.

Fig 5.2 and fig 5.3 show some of the simulated waveforms of the adopted converter in the closed loop in step-up mode for CCM mode of operation.

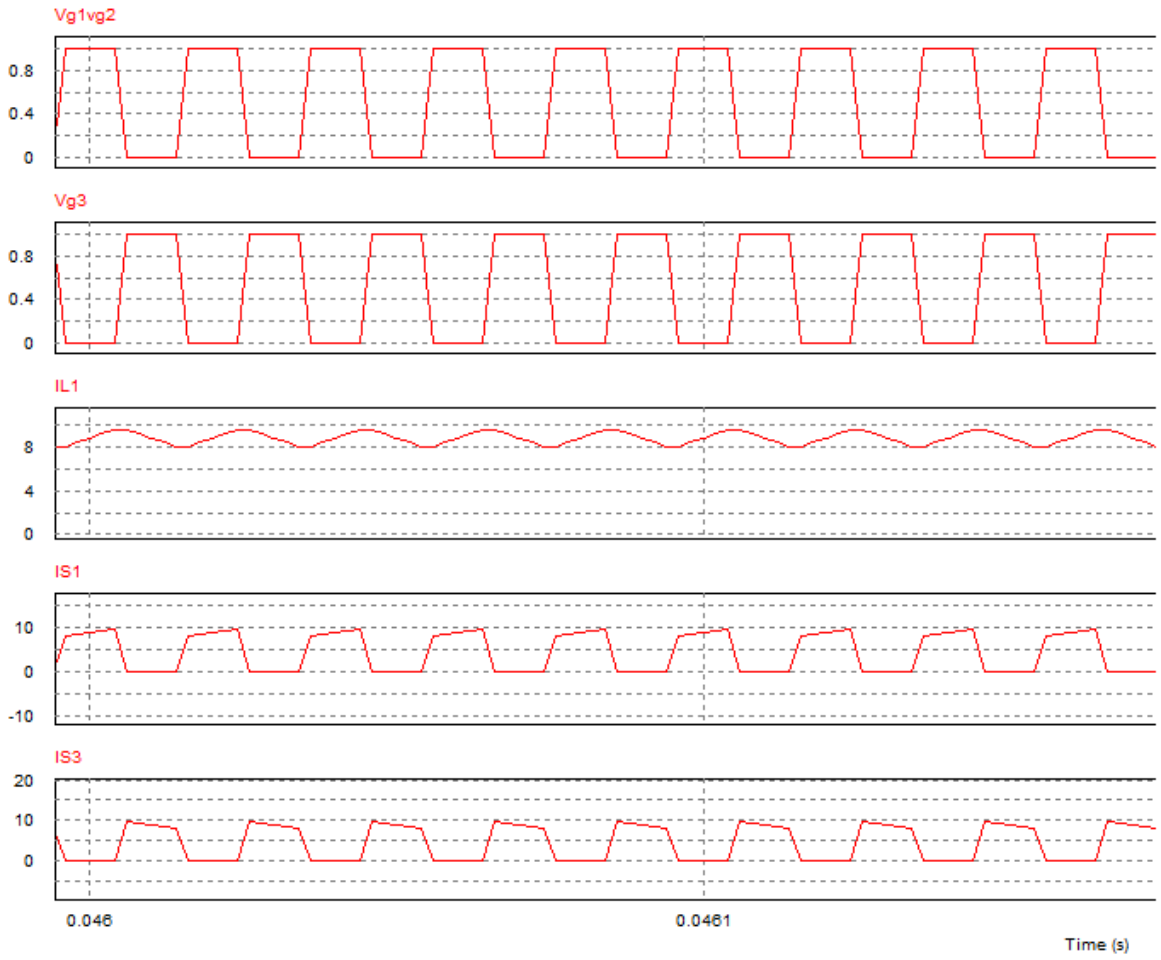

Figure 5.2: Closed loop waveforms in step-up mode- part I

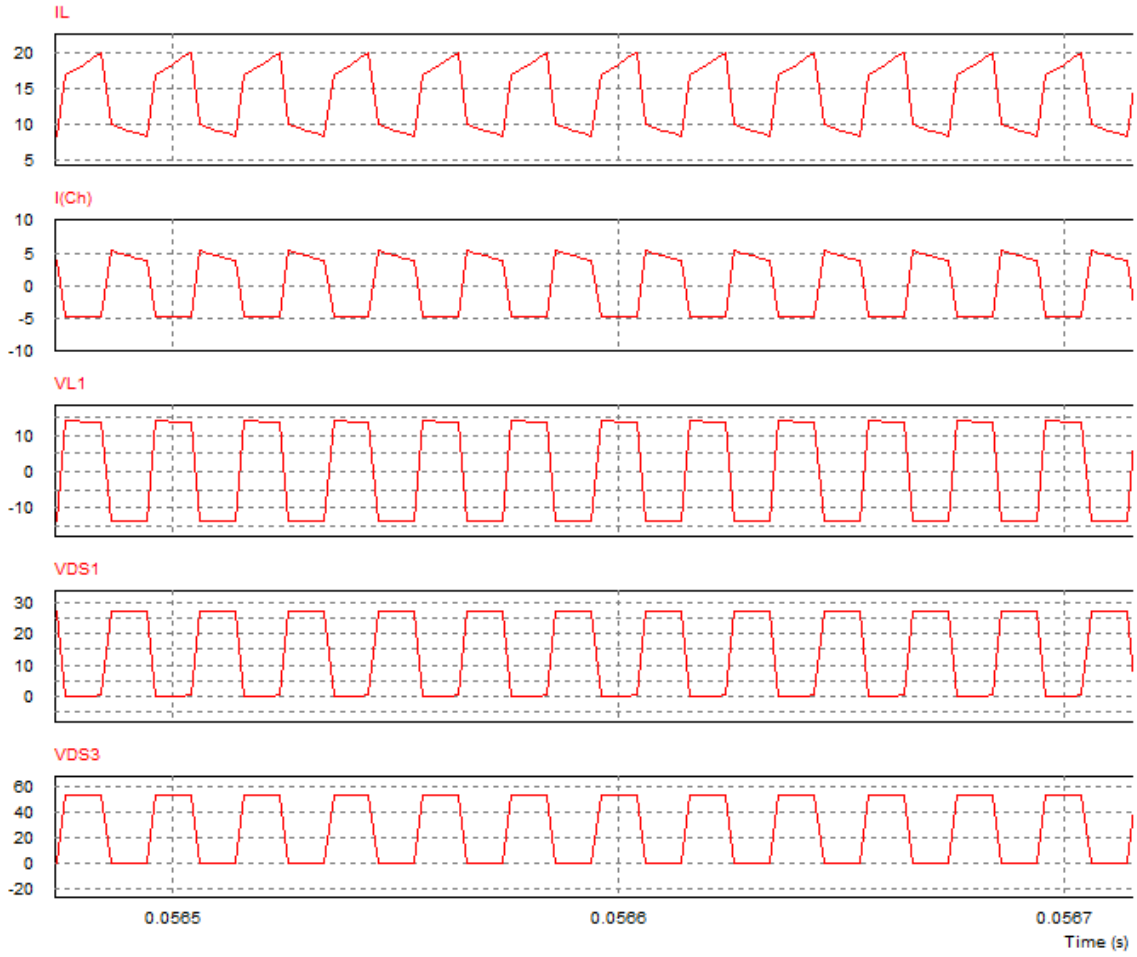

Figure 5.3: Closed loop waveforms in step-up mode-part II

5.2 Step-down Operation

In the closed loop step-down operation too, the circuit parameters and specifications are kept same as that in the open loop system except that the value of inductor needs to be varied by ensuring the inductor current waveform in CCM mode.

Fig 5.4 and fig 5.5 show some of the simulated waveforms of the adopted converter in the closed loop in step-down mode for CCM mode of operation.

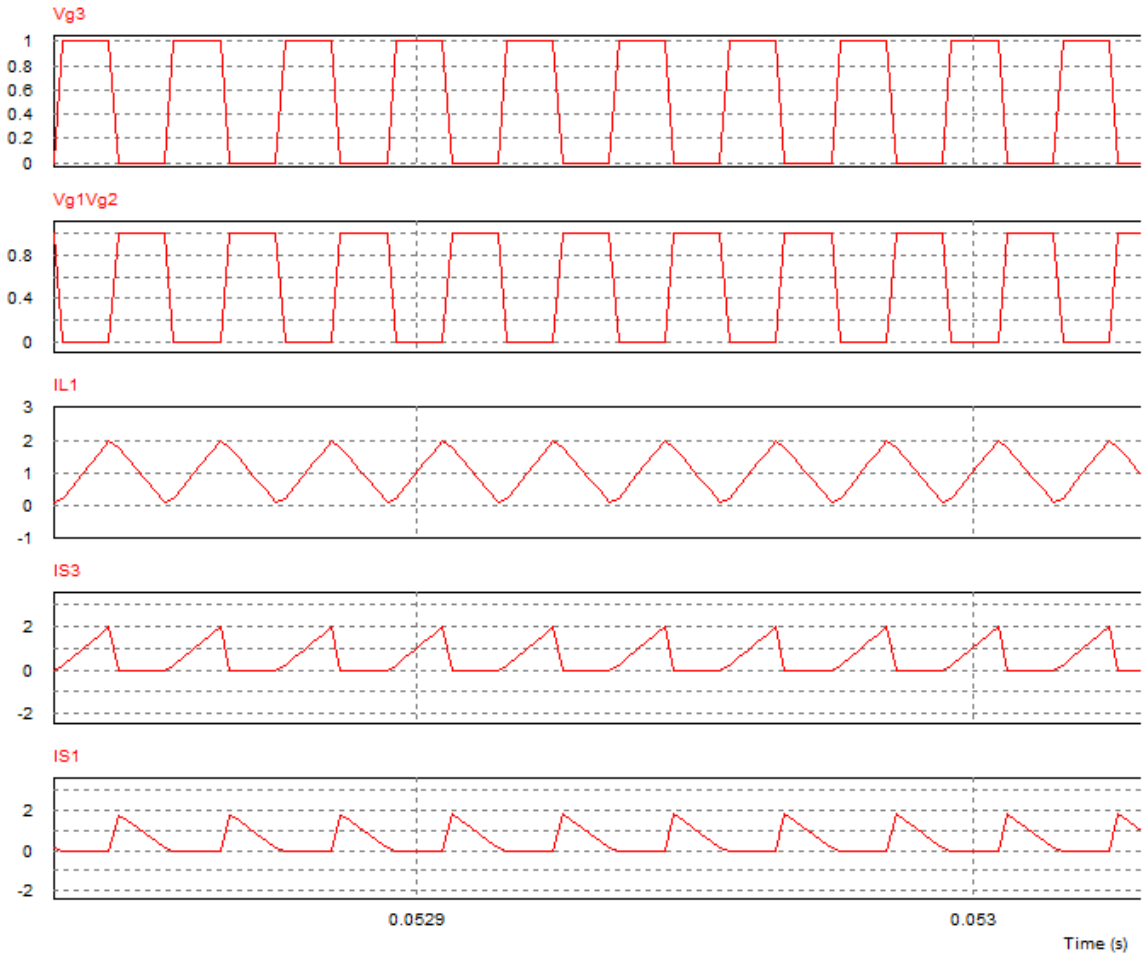

Figure 5.4: Closed loop waveforms in step-down mode-part I

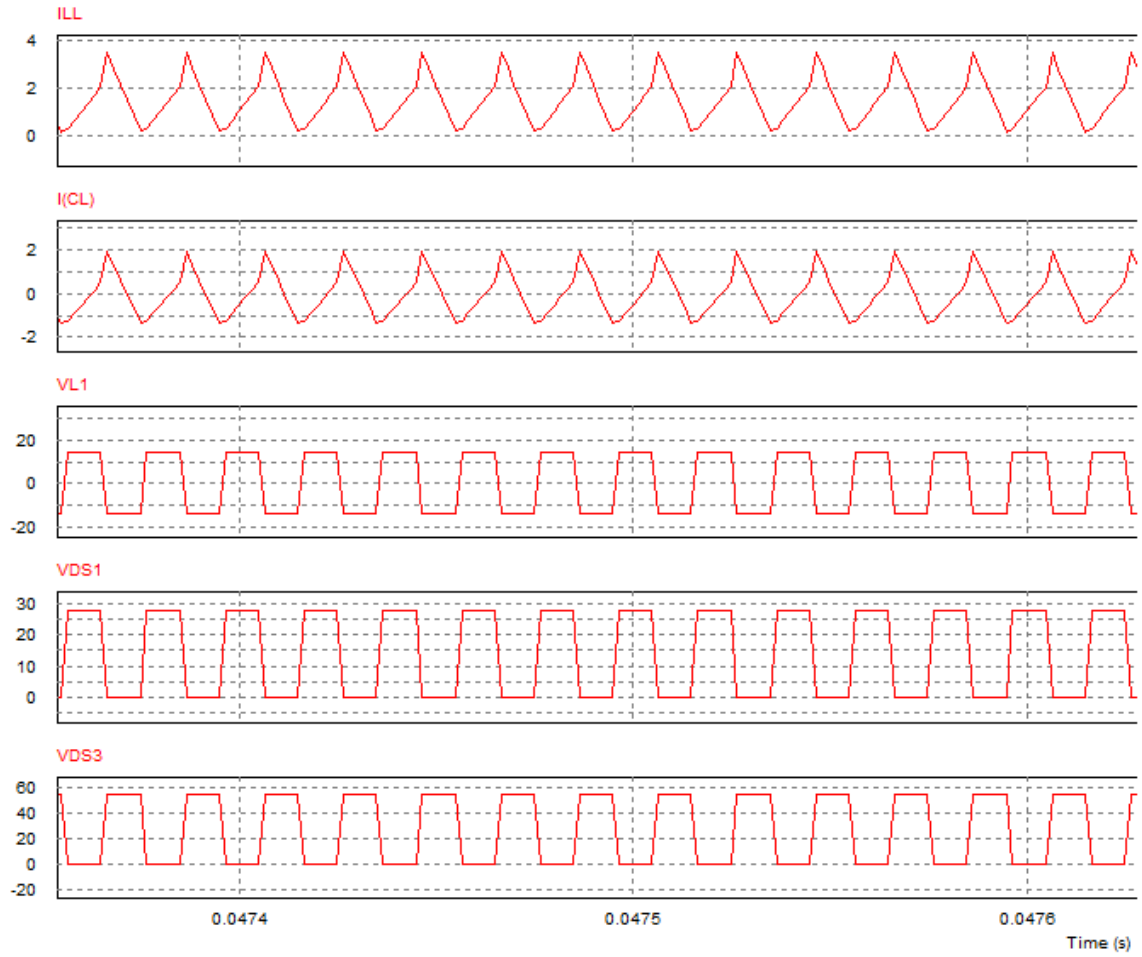

Figure 5.5: Closed loop waveforms in step-down mode-part II

5.3 Simulation for dynamic condition

For bidirectional dc dc converter, a control loop is implemented here. This loop maintains a constant output voltage and determines the duty ratio of the switching converter. The stability of the system depends on the values of the circuit components and the values of the load[10]. If the load varies, the behaviour of system varies. Therefore, a stability analysis is mandatory in order to obtain design guidelines for this kind of dc-dc converter and assure its stability.

At the time of dynamic conditions like overload, the output rated current increases and thus the parameters of the converter are disturbed. So in order to maintain the required voltage at the output of the converter, PI controller loop is implemented and tested with the overload condition.

Here in the simulation, by switching a resistance in parallel with the load resistance for some time, lets say for 0.05 sec, the output current increases and reaches to nearly double the rated value. But the required output voltage of the converter remains constant here due to the implementation of PI Controller. Thus pi loop is tested here and it is working properly.

Fig 5.6 and fig 5.7 show the output current and voltage, inductor current waveforms for this dynamic overload condition.

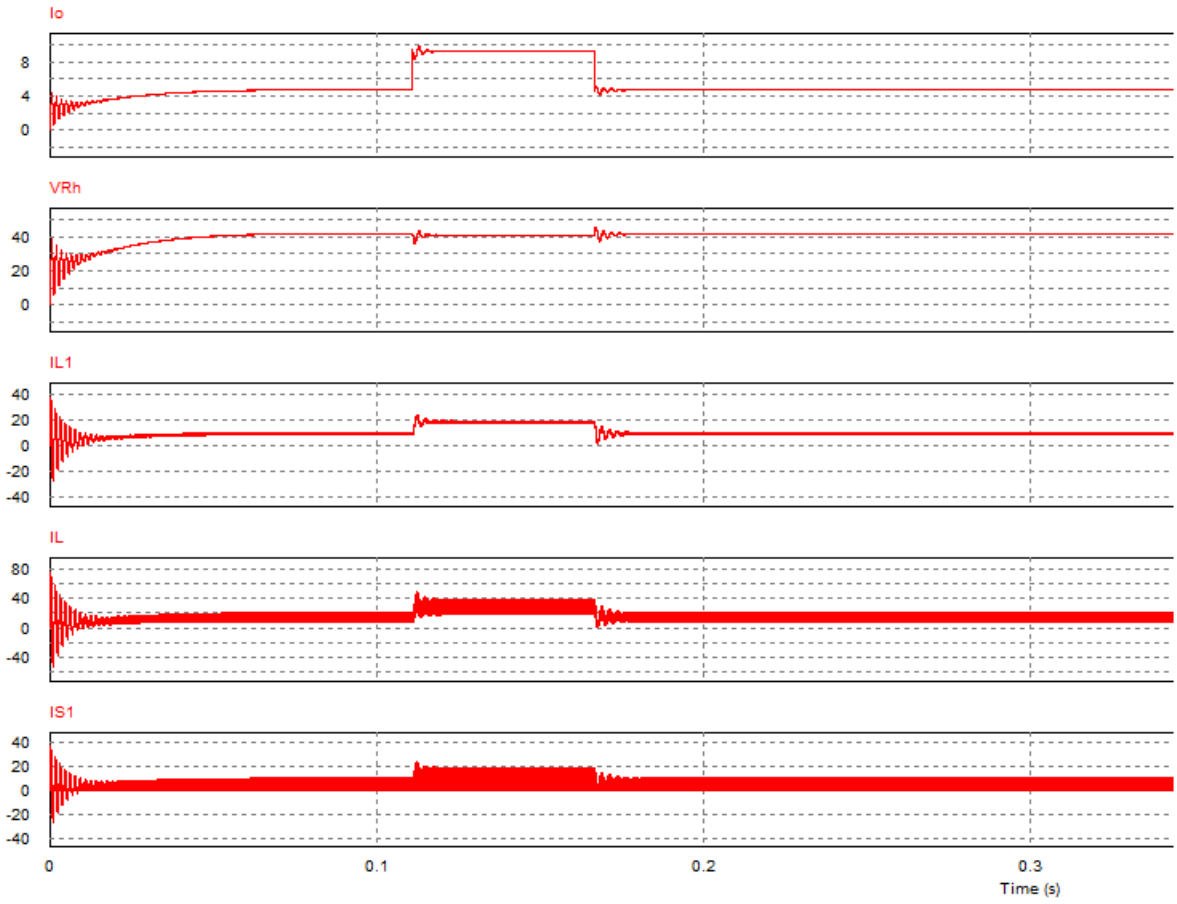

Figure 5.6: Waveforms in step-up mode for overload condition

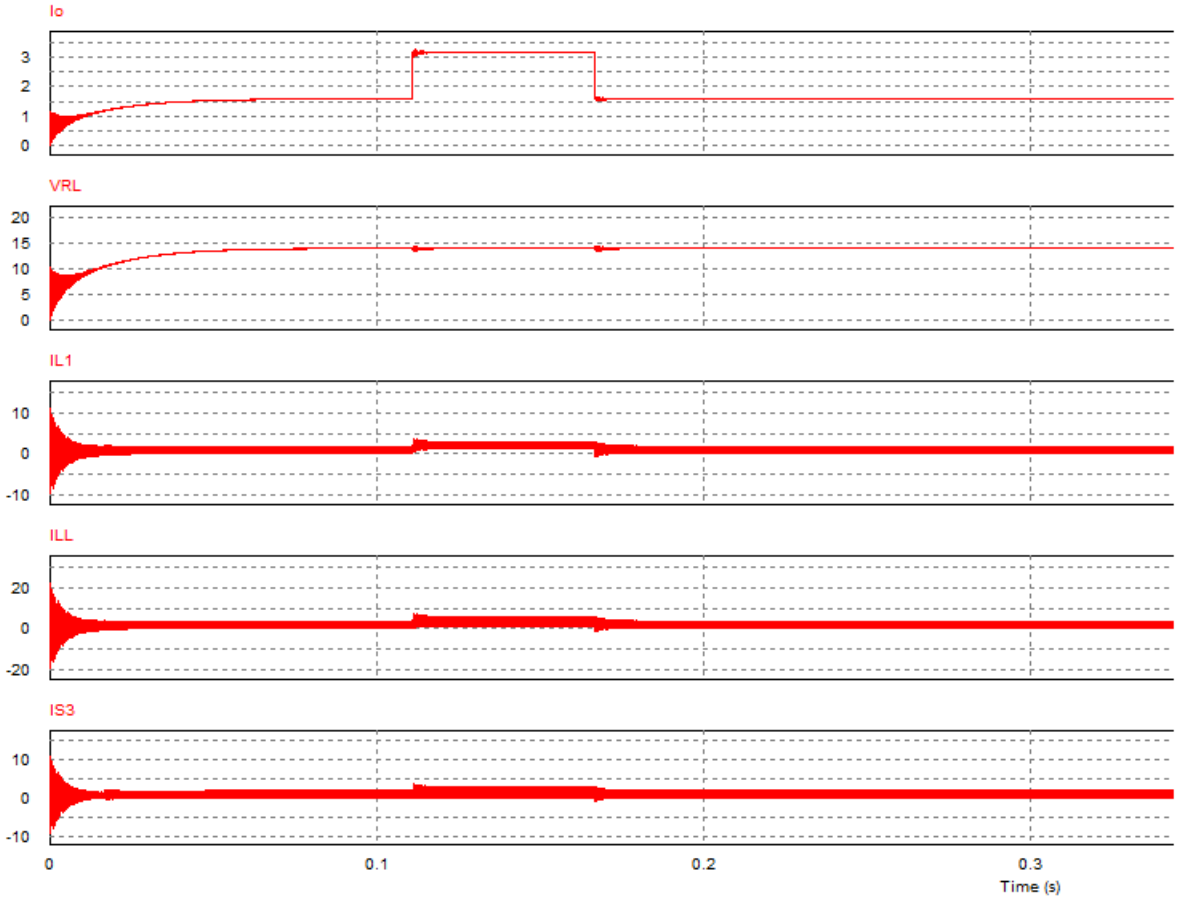

Figure 5.7: Waveforms in step-down mode for overload condition

Chapter 6

Design of the Coupled Inductor

In this chapter, we will cover the basic design steps of coupled inductor, necessary equations and calculations needed when designing a magnetic inductor or coupled inductor. A flyback magnetic is also known as a coupled inductor because it stores energy in one half-cycle and then delivers the energy to the secondary on the next half-cycle, whereas transformers receive and deliver energy to the secondary within the same cycle[13]

Coupled magnetics and coupled filters like coupled inductor can provide smoothing in power converter applications.[12] Unlike most networks, coupled-inductor techniques involve simultaneous parallel energy-transfer pathways: electrical and magnetic. Despite the difficulty, the circuits are useful and deserve to be better appreciated.

From the simulation results in the step-up and step down mode for CCM operation, we know that the value of the coupled inductance at 50kHz is chosen as: $L_1 = L_2 = 35\mu H$. Also mutual inductance $M = 33\mu H$. So coupling coefficient is $k = \frac{M}{\sqrt{L_1 L_2}} = 0.94$.

But while implementing practically in the hardware circuit, which is operating at 20kHz switching frequency of the driver, the value of the inductance has to be increased to operate the converter in CCM mode. Otherwise with the same value of L taken in simulation, while decreasing the frequency, the inductor current waveform goes into DCM mode as it crosses zero point. Thus discontinuity increases when switching frequency decreases. So, in the practical circuit, decreasing the frequency to 20kHz, the value of inductance has to be increased to $140\mu H$ i.e. $0.140mH$.

6.1 Design Procedure for $f_s = 50kHz$ and $L = 35\mu H$

Before starting the design, we must obtain a specification that includes inductance, turns ratio, peak and RMS currents through inductor, output power, and frequency. From the step-up simulation results, we get the following data:
For 200W load and $R_L = 8.82\Omega$,
Rms value of the current flowing through inductor winding $I_{L1} = I_{L2} = 9.3A = I_{rms}$.
Peak to peak ripple current through inductor $\Delta I = 1.6A$
So max value of the inductor current(peak)$I_{max} = I_{peak} = \sqrt{2}I_{rms} = 13.15A$.
Total full load current $I_{FL} = \frac{P_o}{V} = \frac{200W}{42V} = 4.7A$.

6.1.1 Selection of the Proper Core Size

Referring to the design procedure, core selection is facilitated by calculating the core area product (AP) required by the application, and relating this calculation to the APs of available cores.
The core area product A.P is the magnetic cross section area times the window area. Some manufacturers call this WaAc, others AwAe.[14]
At low frequencies, core size is dictated by Cu losses in the windings and the satu-

ration flux density of the core material. At high frequencies, core losses dominate. The core cannot be operated anywhere near saturation flux density .Different AP calculations are required for these two cases. Since the high frequency ripple current is small in this coupled inductor application, the saturation limited case applies. The saturation limited formula is

$$A.P = (\frac{LI_{pk}I_{FL}10^4}{420K_wB_{max}})^{1.31}cm^4 \tag{6.1}$$

where B_{max} for ferrite core material is taken to be $0.3(10^{-4})Wb/cm^2$ and K_w is the core window utilization factor, taken to be 0.5 in this case with two windings. Using the values of this application,

$$A.P = (\frac{35 * 10^{-6} * 13.15 * 4.7}{420 * 0.5 * 0.3 * 10^{-4}})^{1.31}cm^4 = 0.25cm^4 = 0.25(10^4)mm^4 \tag{6.2}$$

An A.P of $0.25(10^4)$ is very small core. So we select EE 42/21/15 core with an A.P of $4.659(10^4)mm^4$ which can satisfy the requirement.

Area Product A.P is the product of window area A_w and magnetic core cross section area A_e.

Referring to the physical, electrical and magnetic properties of ferrite core for EE CORE given in the Ref[11],also in Appendix A, the core parameters are as follows:

Area Product A.P : $4.659(10^4)mm^4$

Magnetic cross-section area, Ae: $182mm^2$

Winding window area, Aw: $256mm^2$

Mean length per turn, MLT: $93mm$

6.1.2 Calculation of no. of turns

The next step is to calculate the minimum number of turns that will take the core to B_{max} at the peak current limit.

$$N_{min} = \frac{LI_{pk}}{B_{max}A_e} \tag{6.3}$$

So, taking B as $0.3 * 10^{-6} Wb/mm^2$ and A_e also in mm,

$$N_{min} = \frac{35 * 10^{-6} * 13.15}{0.3 * 10^{-6} * 182} = 9 turns \tag{6.4}$$

Here $N_1 = N_2 = N$

Using the minimum number of turns, next calculate the center-pole gap length required to achieve the desired inductance L. Relative permeability, μ_r, equals 1 in the gap.

$$l_{gap} = \frac{\mu_0 \mu_r N^2 A_e}{L} m \tag{6.5}$$

So, taking $\mu_0 = 4\Pi * 10^{-7} H/m$ and A_e also in m^2,

$$l_{gap} = \frac{4\Pi * 10^{-7}(1) * 9^2 * 182 * 10^{-6}}{35 * 10^{-6}} = 5.3 * 10^{-4} m = 0.53 mm \tag{6.6}$$

The gap must be placed entirely in the center-leg. The outer legs should be in intimate contact. The amount of leakage inductance is determined by the spacing between the windings.

6.1.3 Selection of wire gauge

To determine the proper gauge of wire, first select the cross section area (a) of wire.

$$a = \frac{I_{rms}}{J} mm^2 \tag{6.7}$$

where J is the current density to be taken as $3.0(10^6) A/m^2$ and
I is the rms current through the inductor.

So,

$$a = \frac{9.3}{3} mm^2 = 3.1 mm^2 \tag{6.8}$$

Now according to this value of a choose the gauge of the wire from SWG wire size table given in the Ref[11] or Appendix B. So SWG 14 is selected which has area $a = 3.24 mm^2$.

Also the window area of the core should accomodate N turns of wire having cross section area (a). Thus following condition is satisfied:

$$K_w A_w \geq (N_1 a + N_2 a) \tag{6.9}$$

or else repeat the calculations for the no. of turns and gauge of wire after choosing the next bigger core.

Figure 6.1 below shows the above designed coupled inductor.

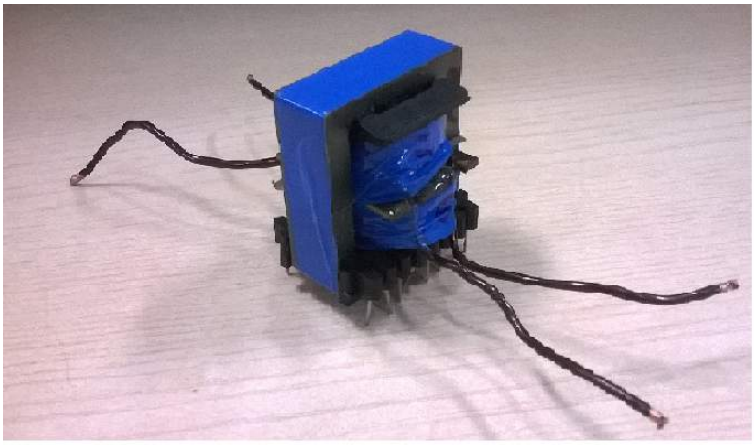

Figure 6.1: Designed coupled inductor

6.2 Design Procedure for $f_s = 20kHz$ and $L = 140\mu H$

The design procedure is same as in above mentioned steps. For $L = 140\mu H$ and keeping all other quantities as same and applying same equations, we get the area product as

$$A.P = (\frac{140 * 10^{-6} * 13.15 * 4.7}{420 * 0.5 * 0.3 * 10^{-4}})^{1.31} cm^4 = 1.515 cm^4 = 1.5(10^4) mm^4 \tag{6.10}$$

An A.P of $1.5(10^4)$ is very small core. So we select EE 42/21/20 core with an A.P of $6.016(10^4) mm^4$ which can satisfy the requirement.

Referring to the physical, electrical and magnetic properties of ferrite core for EE CORE given in Appendix A, the core parameters are as follows:

Area Product A.P : $6.016(10^4) mm^4$

Magnetic cross-section area, Ae: $235 mm^2$

Winding window area, Aw: $256 mm^2$

Mean length per turn, MLT: $99 mm$

The next step is to calculate the minimum number of turns

$$N_{min} = \frac{140 * 10^{-6} * 13.15}{0.3 * 10^{-6} * 235} = 26 turns \tag{6.11}$$

Here $N_1 = N_2 = N = 26$

Now, for testing with the lower rating of load current, let's select the gauge 21 from SWG wire size table given in Appendix B. So SWG 21 is selected which has area $a = 0.518 mm^2$.

Also the window area of the core should accomodate N turns of wire having cross section area (a). Thus the condition $K_w A_w \geq (N_1 a + N_2 a)$ is also satisfied:

Figure 6.2 below shows the coupled inductor designed at 20 kHz.

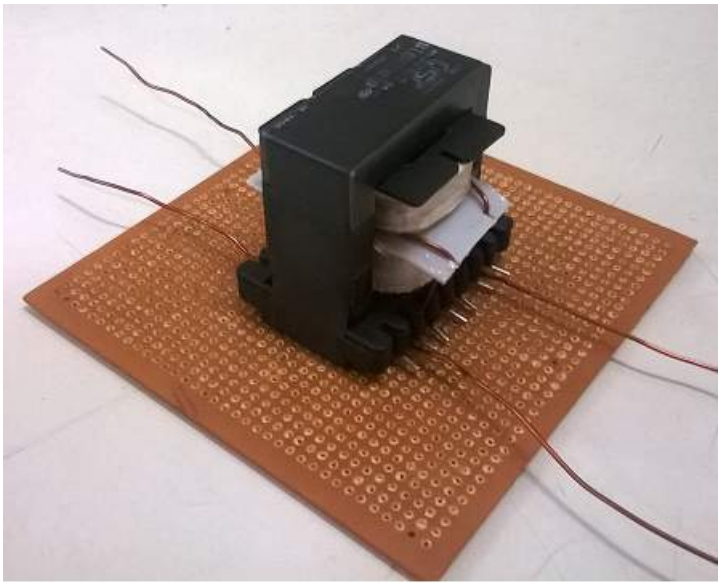

Figure 6.2: Designed coupled inductor at 20 kHz

Chapter 7

Simulation at reduced frequency

Here in this chapter, simulation is done in the open loop mode at reduced frequency of 20 kHz.

While implementing in the practical circuit, at this reduced frequency, we know that the value of inductance has to be increased and is taken as $L = 140\mu H$ and $M = 130\mu H$ to get the simulation results in CCM mode . So considering this value of L, the voltage and current waveforms are verified to have continuous current. All other simulation parameters/specifications are kept same as in the previous chapter 4.

7.1 Step-up Operation

For $L = 140\mu H$, $M = 130\mu H$ and keeping load resistance as $R = 100\Omega$, fig 7.1 and fig 7.2 show some of the simulated waveforms of the adopted converter in step-up mode at 20 kHz for CCM mode of operation.

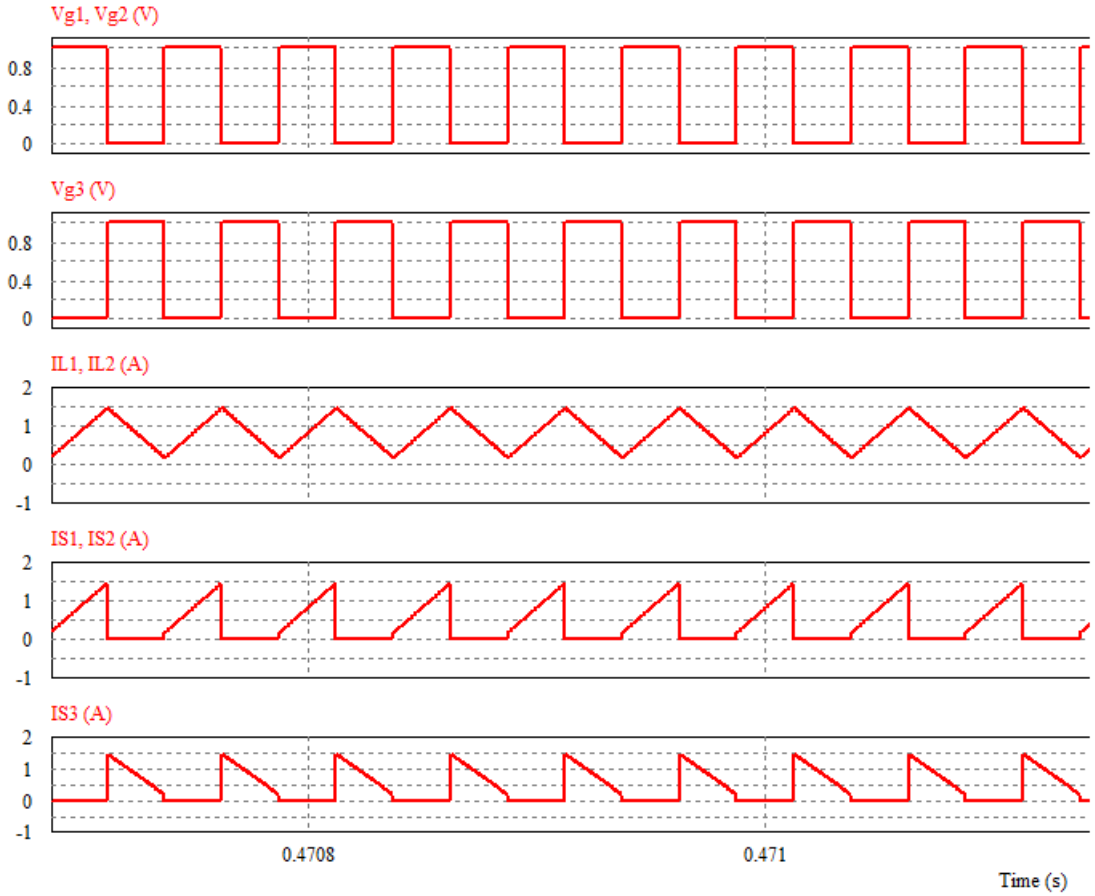

Figure 7.1: Waveforms at 20 kHz in step-up mode-part I

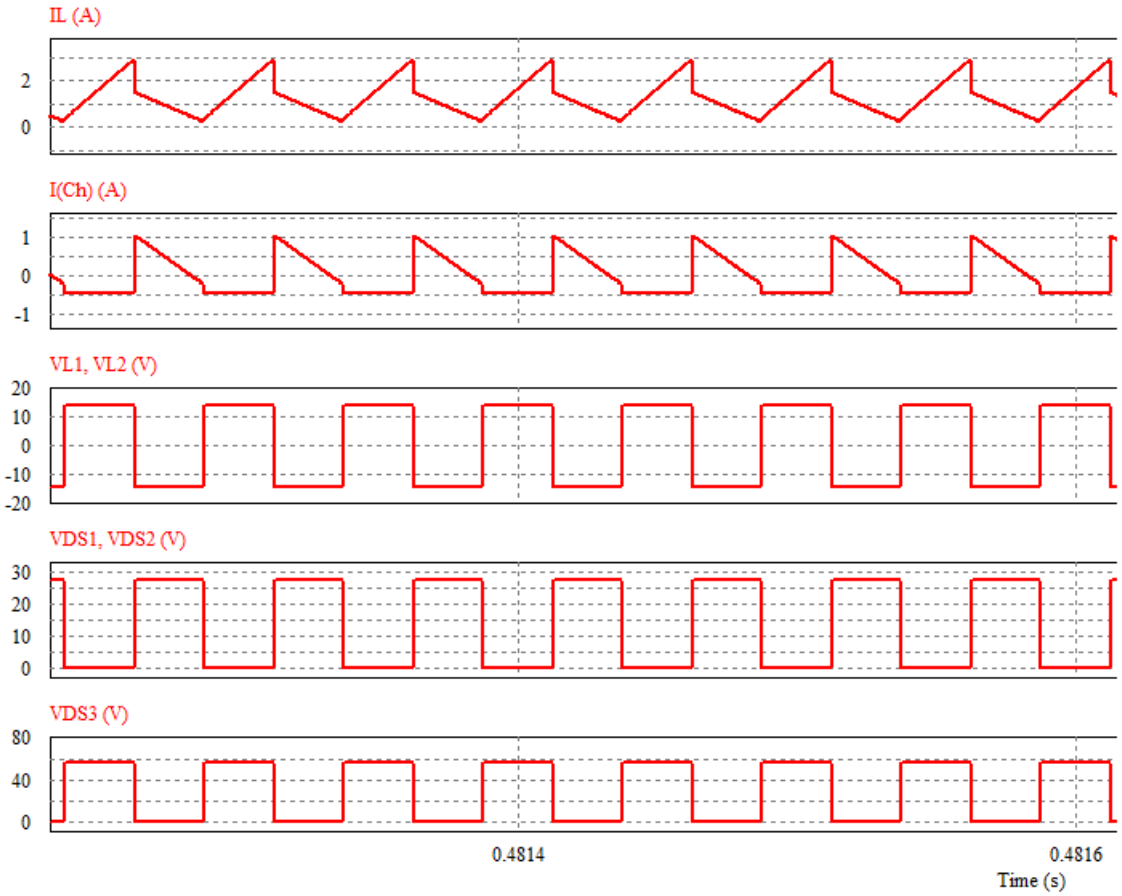

Figure 7.2: Waveforms at 20 kHz in step-up mode-part II

7.2 Step-down Operation

For $L = 140\mu H$, $M = 130\mu H$ and keeping load resistance as $R = 8.82\Omega$, fig 7.3 and fig 7.4 show some of the simulated waveforms of the adopted converter in step-down mode at 20 kHz for CCM mode of operation.

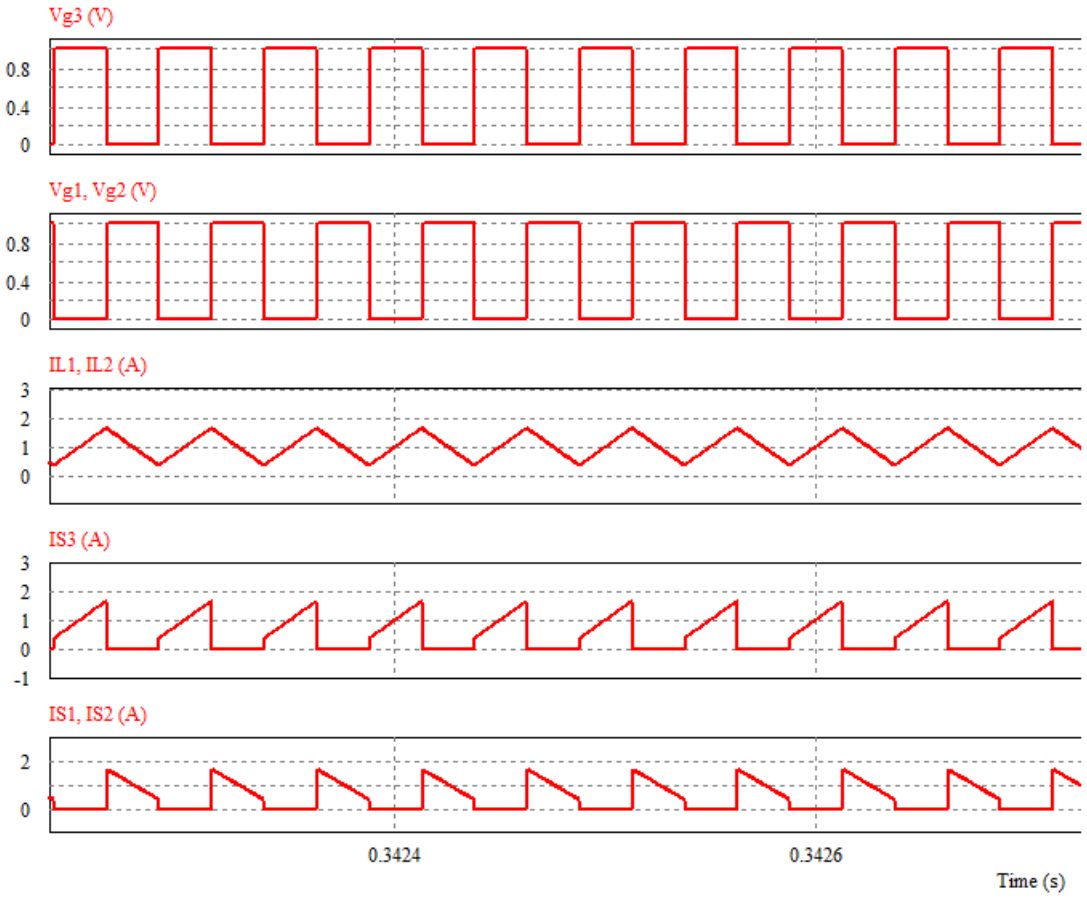

Figure 7.3: Waveforms at 20 kHz in step-down mode-part I

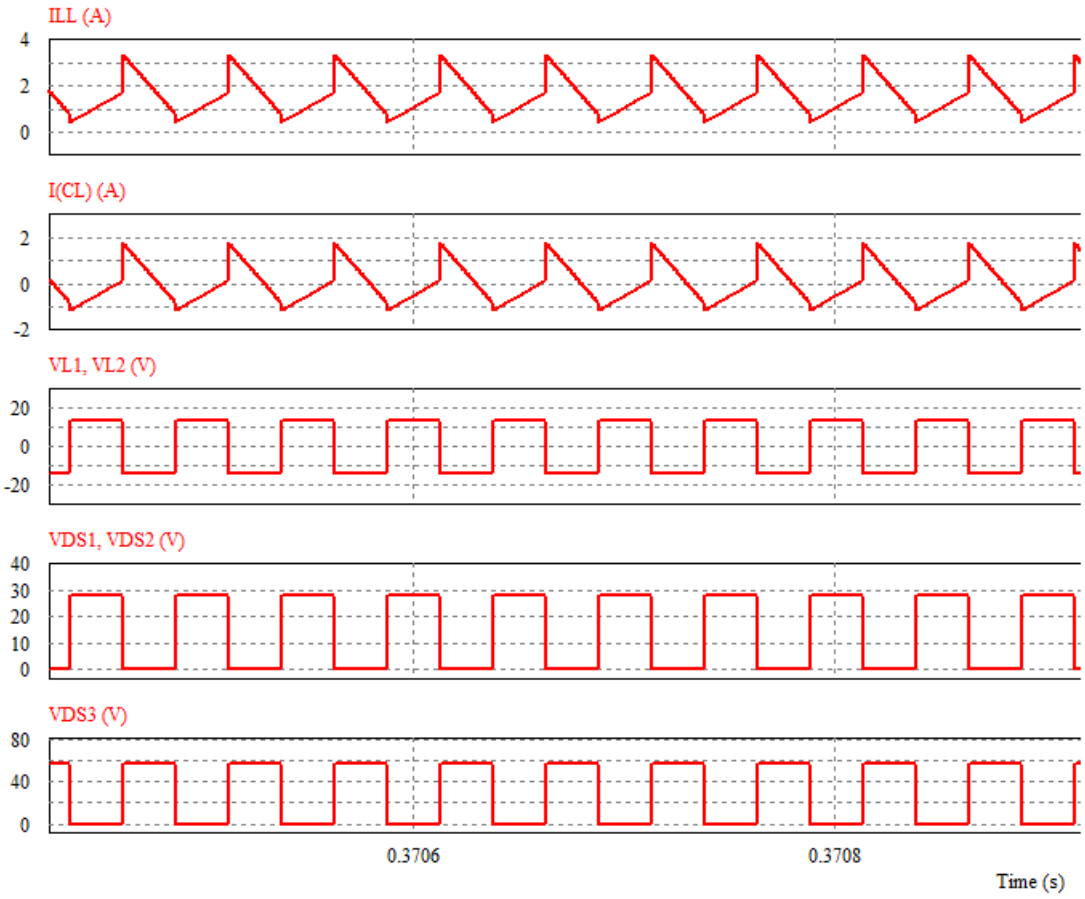

Figure 7.4: Waveforms at 20 kHz in step-down mode-part II

Chapter 8

Driver circuit Implementation

The gate driver circuit is an integral part of any power converter. The characteristics of the gate driver circuits are the key elements in observing the desired output and the control requirements of any power converters. The gate driver ICs are becoming more commercially available with increasing applications of power electronics.
The gate driver circuits which are of low level provide isolation from the high level power circuits through isolation devices or techniques such as optocouplers and pulse transformers.
Here for driving the Mosfets of the converter, driver IC TLP250 is used.

8.1 Driver Circuit using TLP250

The TOSHIBA TLP250 is an optocoupler driver IC which consists of a GaAlAs light emitting diode and a integrated photodetector. It is suitable for gate driving circuit of IGBT or power MOSFET. Some of the important specifications of TLP250 are as follows:
Input threshold current $I_F : 5mA(max.)$
Supply current $(I_{CC}) : 11mA(max.)$

Supply voltage (V_{CC}) : $10 - 35V$
Output current (I_O) : $1.5A(max.)$
Switching time (t_{pLH}/t_{pHL}) : $1.5\mu s(max)$.
Isolation voltage : $2500V_{rms}(min.)$
Operating frequency f : $25kHz$

As mosfet is a voltage controlled device, applying a gate voltage turns it on and it draws negligible gate current. The gate drive circuit should have low impedance for fast turn-on. Mosfets have very high input impedance. To achieve switching speeds of order of 100 ns or less, the gate drive circuit should have a low output impedance and the ability to sink and source relatively large currents.

Thus a totem-pole arrangement of driver IC TLP250, that is capable of sourcing and sinking a large current, is used. The pnp and npn transistors act as emitter followers and offer a low output impedance. These transistors operate in the linear region instead of the saturation mode, thereby minimizing the delay time.

The figure 8.1 below shows the driver circuit using TLP250 which drives the Mosfet and provides isolation between control circuit and power circuit. Three separate power supplies are also required for the three driver ICs, for each of the Mosfet.

As shown in the circuit diagram of TLP250, control pulse of 5V having 20kHz frquency and duty ratio of 0.5, from the Arduino Uno controller, is given to the pin no 2 which is anode, and a resistance of 1k ohm is connected for the protection purpose. The control ground is connected at pin no 3 which is cathode. The pin no 8 is Vcc, which gets the supply voltage of 15 V from a separate power supply. A ceramic capacitor of $0.1\mu F$ is connected between pin no. 8 and 5. The output gate pulse of 15V is obtained at pin no 6, according to the amount of Vcc supplied. Also 1k

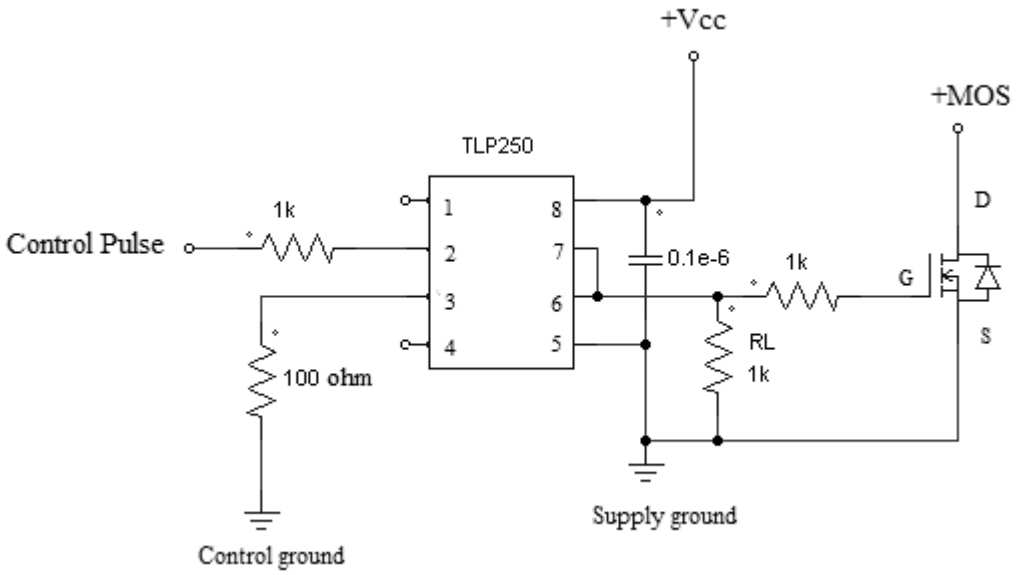

Figure 8.1: Driver circuit using TLP250

ohm resistance is connected at the output pin of driver which goes to the gate of the Mosfet to limit the gate current and similar value for the load resistance between pin no 6 and pin no 5 which is the supply ground. The supply ground is connected to the source of the Mosfet.

Figure 8.2 shows the output of the driver circuit i.e the gate pulses applied to Mosfets. The inverted gate pulse is obtained by giving inverted control logic to the driver, through the NOT gate IC7404.

8.2 Power Supply for the driver circuit

A 15 V power supply is made for each of the driver circuit. In the power supply circuit as shown the fig 8.3, $230V$ A.C. supply from the mains is stepped down to $15V$ A.C. through a centre taped transformer having rating $15-0-15V$, 1 Amp, which is then rectified with the help of a diode bridge rectifier and filtered through a $1000\mu F$, $25V$ capacitor. This unregulated output of the rectifier is then fed to the voltage regulator IC LM7815 to obtain a regulated $15V$ D.C. supply.

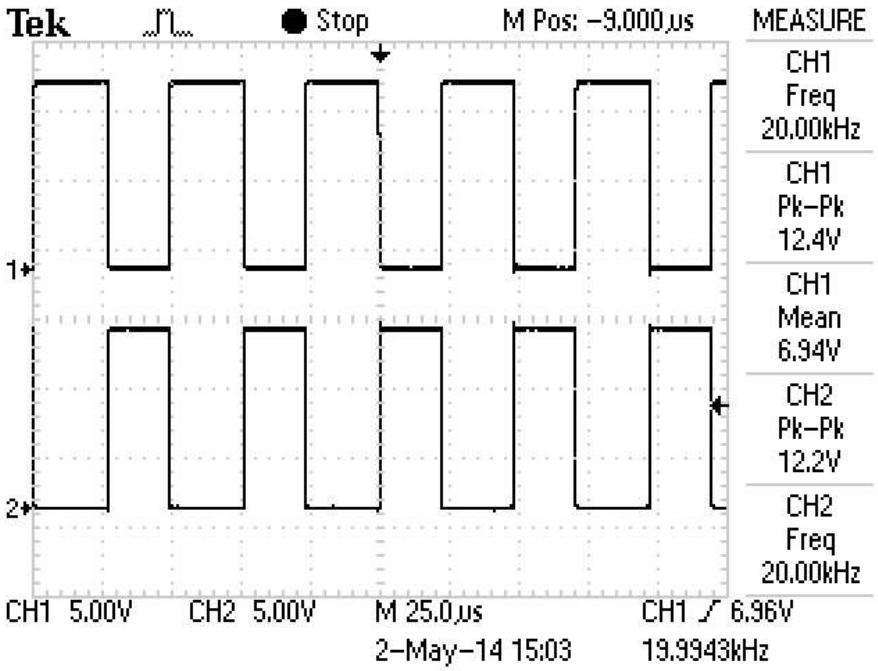

Figure 8.2: High and low Gate pulses for Mosfet

Figure 8.3 below shows the power supply circuit diagram.

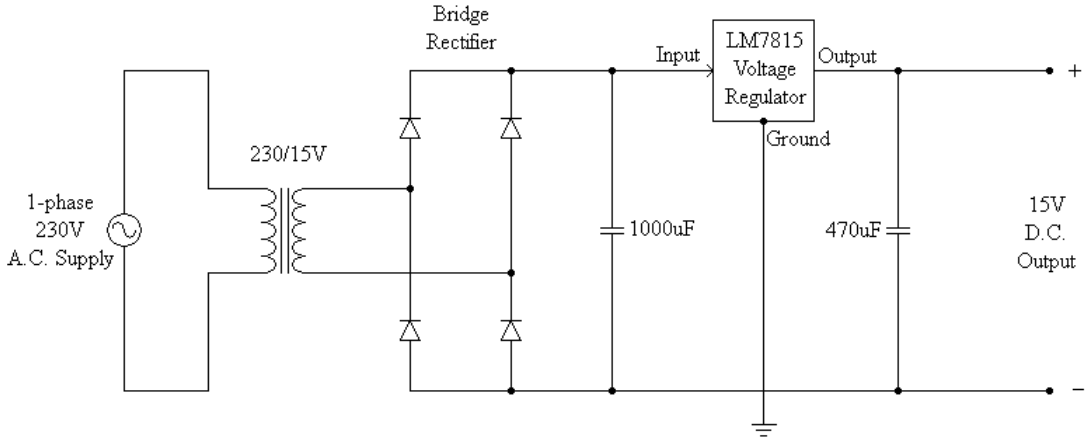

Figure 8.3: Power supply circuit for gate driver

The figure 8.4 below shows the driver card prepared.

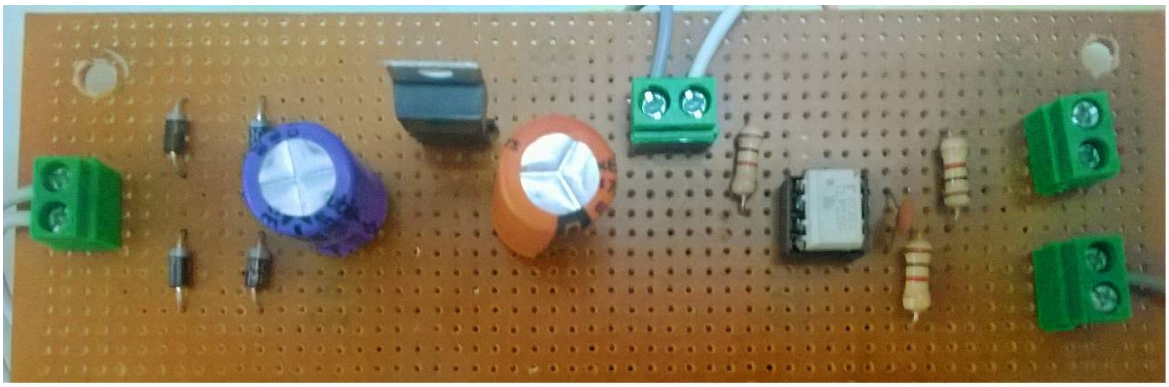

Figure 8.4: Gate Driver Card

Chapter 9

Programming through Controller

9.1 Introduction to Arduino

To obtain required control pulses, Arduino controller is used.
Arduino is a tool for making computers that can sense and control more of the physical world than our desktop computer. It's an open-source physical computing platform based on a simple microcontroller board, and a development environment for writing software for the board. The development of language and development environment is very simple, easy to understand, very suitable for beginners to learn.

9.1.1 Arduino Uno R3

The Arduino Uno is a microcontroller board based on the ATmega328. It has 14 digital input/output pins (of which 6 can be used as PWM outputs), 6 analog inputs, a 16 MHz ceramic resonator, a USB connection, a power jack, an ICSP header, and a reset button. It contains everything needed to support the microcontroller; simply connect it to a computer with a USB cable or power it with a AC-to-DC adapter or battery to get started. Revision 3 is the last SainSmart UNO development board

version. Some of the features of Arduino Uno are mentioned as follows:

Working voltage 3.3V/5V is optional.

Operating voltage of arduino is 5 V.

Input voltage limit is 6-20 V.

Input voltage (recommended) is 7-12 V DC.

Current per i/o pin is 40 mA.

5V Electric current is 500mA.

Flash memory is 32 KB of which 0.5 KB used by bootloader.

SRAM is 2 kB

EEPROM is 1 kB

Clock speed is 16 MHz.

Figure 9.1: Front view of Arduino Uno

9.2 Programming Description

A PWM signal is generated through programming. Pulse Width Modulation is a technique for getting analog results with digital means. Digital control is used to

create a square wave, a signal switched between on and off. This on-off pattern can simulate voltages in between full on (5 Volts) and off (0 Volts) by changing the portion of the time the signal spends on versus the time that the signal spends off. The duration of "on time" is called the pulse width. To get varying analog values, we can change or modulate that pulse width.

In the figure 9.2 below, the green lines represent a regular time period. This duration or period is the inverse of the PWM frequency. In other words, with Arduino's PWM frequency at about lets say $500Hz$, the green lines would measure 2 milliseconds each. A call to pwmWrite() is on a scale of 0 - 255, such that pwmWrite(255) requests a 100 percent duty cycle (always ON), and pwmWrite(127) is a 50 percent duty cycle (ON half the time) for example.

The syntax function of pwmWrite is same as analogWrite. For the Arduino, we

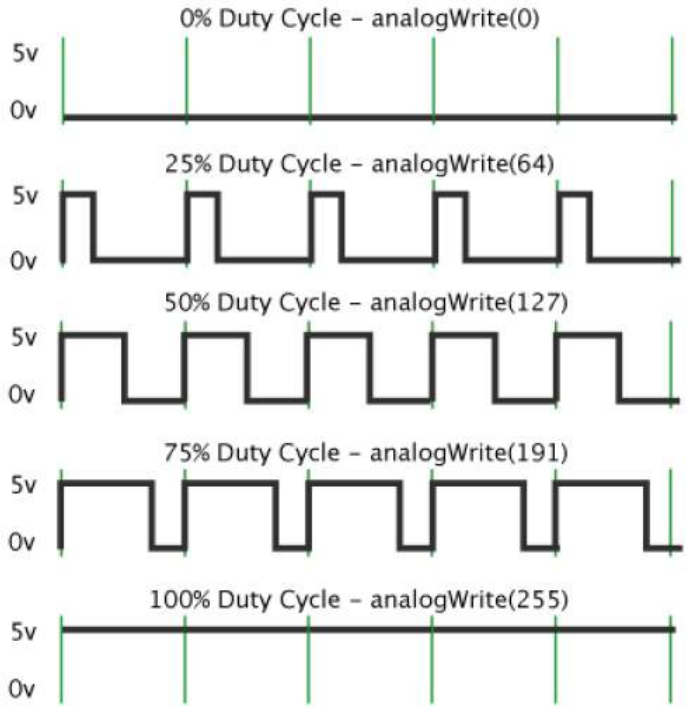

Figure 9.2: PWM Technique in Controller

write a value from 0 to 255 on a PWM pin, and the Arduino library will cause the pin to output a PWM signal whose ON time is in proportion to the value written.

Thus a pwm frequency library needs to be installed. On most Arduino boards (those with the ATmega168 or ATmega328), the pwm function works on pins 3, 5, 6, 9, 10, and 11.

Also PWM behavior is determined by integrated components called timers. Every timer has two to four channels. Each channel is connected to a pin. Changing one pin's frequency requires changes to the timer it connects to. Which in turn changes the frequency of other pins connected to that same timer. Thus a timer has to be initialised.

Following this procedure, control pulse of 5V, having 50 percent duty cycle and 20kHz frequency is generated as shown in the figure 9.3 and by inserting a NOT gate, its inverted pulse can be obtained.

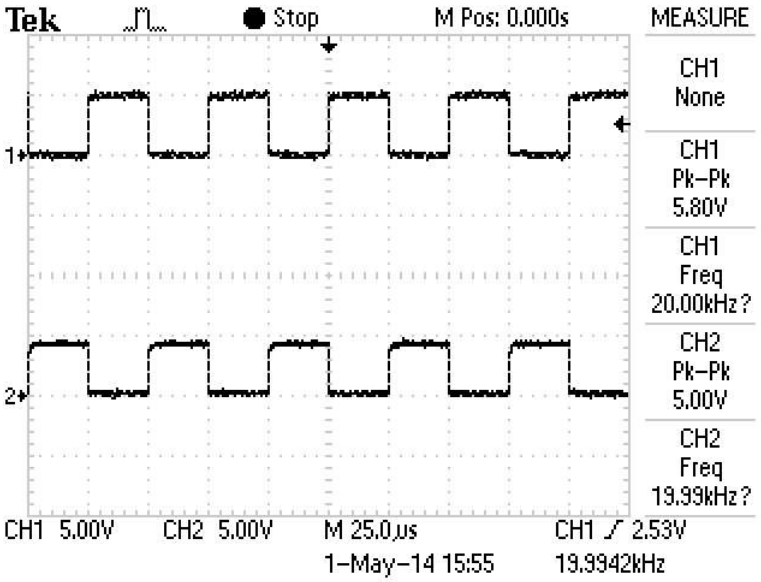

Figure 9.3: Control pulse at 20kHz

Chapter 10

Testing the Hardware Set-up

The whole Converter system integration is shown in the figure 10.1.

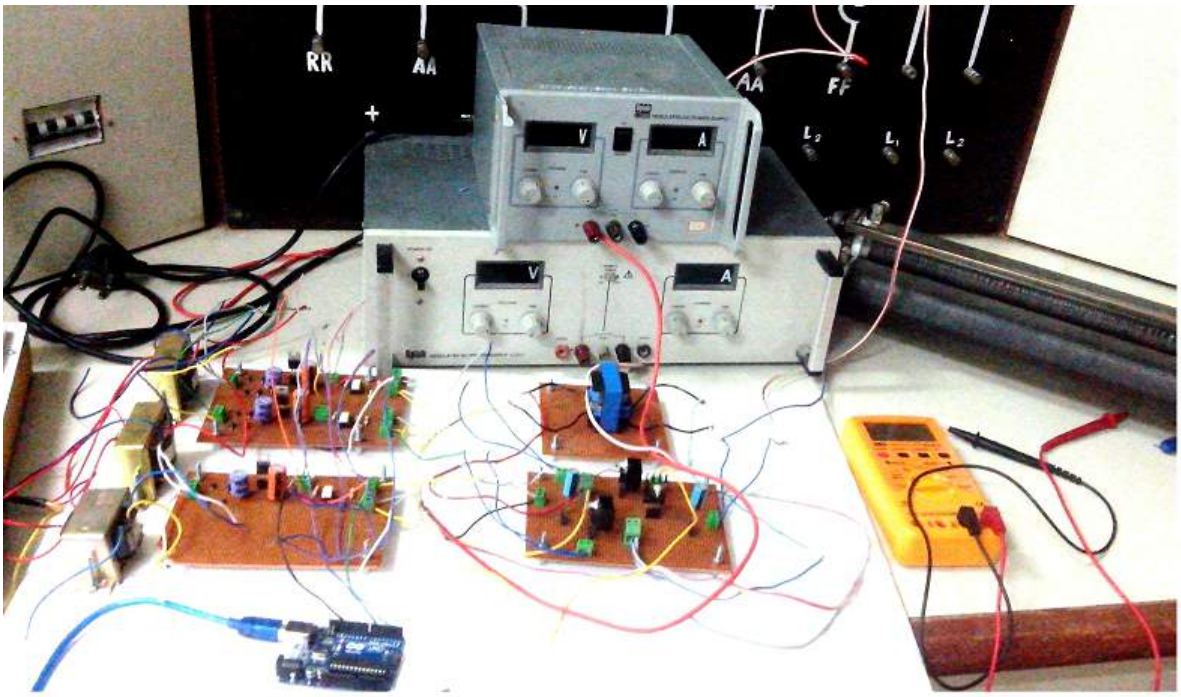

Figure 10.1: The Converter system set-up

The whole hardware set-up includes the power supply circuit, the driver circuit, the

main power circuit with the coupled inductor and the load.

10.1 Power Circuit

In the power circuit, a dc voltage of $14V$ is gradually given to the coupled inductor winding having actual practical inductance as $L_1 = 119\mu H$ and $L_2 = 148\mu H$ and then the current flow through the switches S_1, S_2 and S_3 according to the switching pattern, is followed. A capacitance of $330\mu F$ and rheostatic load of 100 Ω, 5 A is connected at the load side. Thus the voltage which is stepped up, is measured at the load end.

Similarly, the procedure is followed for step down mode, where input voltage of 42V is to be applied and the output voltage which is stepped down is measured at the load end.

The power circuit set-up is shown in the figure 10.2 below.

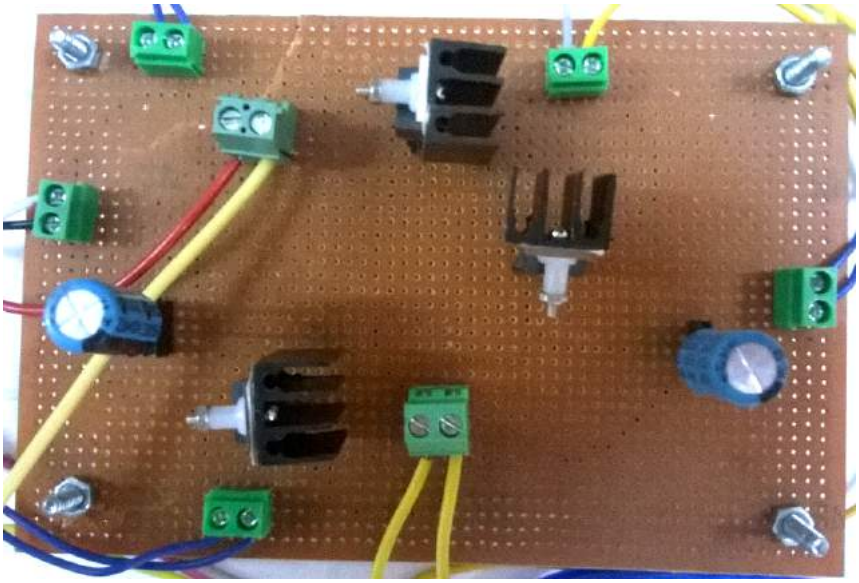

Figure 10.2: Power circuit set-up

10.2 Observation Results

After whole system integration, it is found that when switching ON the driver, the gate pulse of the Mosfet is obtained in the required manner in the power circuit. But at the same time, when the dc voltage of the converter is switched, the system supply goes into overcurrent mode. Thus the problem of the overcurrent is to be troubleshooted. Probably the problem of the coupled inductor may be the cause which can be troubleshooted.

Chapter 11

Conclusion and Future Work

11.1 Conclusion

A bidirectional converter topology is adopted with minimum switches and a coupled inductor. Its operation is studied and the circuit is analysed in step-up and step-down modes. From simulation results in the open loop mode as well as in the closed loop mode, it is observed that the voltage and current waveforms are mostly matched with the theoretical ones. Further in the dynamic condition too, the output of the system remains stable. Also design of the converter is analysed at 50kHz as well as 20kHz frequency. By reducing the frequency to 20kHz for the hardware set-up, the value of the coupled inductor has to be redesigned and tested. After integrating it into the whole system, it is found that the converter goes into the overcurrent mode and thus troubleshooting is to be continued. The control circuit and the driver cicuit results are satisfactory.

11.2 Future Work

The future work in this project includes the following things :

a. To test with the power circuit and troubleshoot the problem of overcurrent.

b. Probably, to overcome the problem of coupled inductor.

c. Implementation of the closed loop system can also be done.

References

[1] Manu Jain,"Bi-directional dc-dc converter for low power application" Concordia University Montral, Qubec, Canada, February 1998.

[2] Mousumi Biswal, Sidharth Sabyasachi,"A Study on Recent DC-DC Converters", International Journal of Engineering Research and Applications (IJERA), November- December 2012, pp.657-663

[3] C.-C. Lin, L.-S. Yang, G.W. Wu, "Study of a non-isolated bidirectional DCDC converter", IET Power Electron., 2013, Vol. 6, Iss. 1, pp. 3037.

[4] N. Mahesh, D. Seshi Reddy, "A Novel of Bidirectional DC-DC converter drive", IJMER, Vol.2, Issue.2, Mar-Apr 2012 pp-186-196..

[5] Hamid R. Karshenas, Hamid Daneshpajooh, et. al."Bidirectional DC-DC Converters for Energy Storage System", Queens University, Kingston, Canada.

[6] Lung-Sheng Yang and Tsorng-Juu Liang, "Analysis and Implementation of a Novel Bidirectional DCDC Converter", IEEE Transactions on Industrial Electronics, vol. 59, no. 1, January 2012.

[7] Srinivas Reddy Gurrala, K.Vara Lakshmi, "A Novel Bidirectional DC-DC Converter with Battery Protection", IJMER, Vol.2, Issue.6, Nov-Dec. 2012 pp-4261-4265.

[8] Su-Won Lee, Seong-Ryong Lee and Chil-Hwan Jeon, "A New High Efficient Bi-directional DC/DC Converter in the Dual Voltage System", Journal of Electrical Engineering & Technology, Vol. 1, No. 3, pp. 343 350, 2006.

[9] Kemal Ari , Faik Tekin Asal , Mert Cosgun, "PI, PD, PID Controllers-EE 402 Discrete Time Sytems Project Report ", Middle East Technical University

[10] Alfonso Conesa, Herminio Martnez and Jose Mara Huerta, "Dynamic Analysis of Hybrid DCDC Converters", Technical University of Catalonia (EUETIB / UPC), C/ Comte dUrgell, 187. E08036. Barcelona, SPAIN

[11] Umanand L, Bhat S.R,"Design of magnetic components for Switched Mode Power Converters", New Age International Publisher, New Delhi, 2001.

[12] Robert Balog, Philip T. Krein, et. al. "Coupled Inductors A Basic Filter Building Block", Dept. of Electrical and Computer Engineering, University of Illinois, Urbana, Illinois, USA.

[13] Louis R. Diana, "Practical Magnetic Design: Inductors and Coupled Inductors".

[14] Lloyd Dixon, "Coupled Inductor Design", Unitrode Corporation, May 93.

[15] Junhong Zhang "Bidirectional DC-DC Power Converter Design Optimization, Modeling and Control", Blacksburg, Virginia, Jan. 30, 2008

Appendix A

Ferrite core properties

Physical, Electrical and Magnetic characteristics of ferrite cores

CORES without air gap	mean length per turn l_t mm	mean magnetic length l_m mm	core cross section area $A_e \times 100$ mm^2	window area $A_w \times 100$ mm^2	area product $A_p \times 10^4$ mm^4	effective relative permeability $\mu_r \pm 25\%$	A_L nH/turns^2 $\pm 25\%$
POTCORES - CEL HP$_3$C grade, (*Philip 3B7 grade)							
P 18/11	35.6	26	0.43	0.266	0.114	1480	3122
P 26/16	52	37.5	0.94	0.53	0.498	1670	5247
P 30/19	60	45.2	1.36	0.747	1.016	1760	6703
P 36/22	73	53.2	2.01	1.01	2.010	2030*	9500*
P 42/29	86	68.6	2.64	1.81	4.778	2120*	10250*
P 66/56	130	123	7.15	5.18	37.03		
EE - CORES - CEL HP$_3$C grade							
E 20/10/5	38	42.8	0.31	0.478	0.149	1770	1624
E 25/9/6	51.2	48.8	0.40	0.78	0.312	1840	1895
E 25/13/7	52	57.5	0.55	0.87	0.478	1900	2285
E 30/15/7	56	66.9	0.597	1.19	0.71		
E 36/18/11	70.6	78.0	1.31	1.41	1.847	2000	4200
E 42/21/9	77.6	108.5	1.07	2.56	2.739	2100	2613
E 42/21/15	93	97.2	1.82	2.56	4.659	2030	4778
E 42/21/20	99	98.0	2.35	2.56	6.016	2058	6231
E 65/32/13	150	146.3	2.66	5.37	14.284	2115	4833

Appendix B

SWG Table

Standard Wire Gauge	Diameter		Turns of wire		Cross-sectional area		Res. per length (for copper wire)		Mass per length		Current Capacity / A	
	in	mm	in^{-1}	mm^{-1}	kcmil	mm^2	Ω/km	Ω/kft	lb/ft	kg/m	750 kcmil/A	500kcmil/A
0000000 (7/0)	0.500	12.7	2.00	0.0787	250	127	0.136	0.447	0.759	1.13	333	500
000000 (6/0)	0.464	11.8	2.16	0.0848	215	109	0.158	0.519	0.654	0.973	287	431
00000 (5/0)	0.432	11.0	2.31	0.0911	187	94.6	0.182	0.598	0.567	0.844	249	373
0000 (4/0)	0.400	10.2	2.50	0.0984	160	81.1	0.213	0.698	0.486	0.723	213	320
000 (3/0)	0.372	9.45	2.69	0.106	138	70.1	0.246	0.807	0.420	0.625	185	277
00 (2/0)	0.348	8.84	2.87	0.113	121	61.4	0.281	0.922	0.368	0.547	161	242
0 (1/0)	0.324	8.23	3.09	0.122	105	53.2	0.324	1.06	0.319	0.474	140	210
1	0.300	7.62	3.33	0.131	90.0	45.6	0.378	1.24	0.273	0.407	120	180
2	0.276	7.01	3.62	0.143	76.2	38.6	0.447	1.47	0.231	0.344	102	152
3	0.252	6.40	3.97	0.156	63.5	32.2	0.536	1.76	0.193	0.287	84.7	127
4	0.232	5.89	4.31	0.170	53.8	27.3	0.632	2.07	0.163	0.243	71.8	108
5	0.212	5.38	4.72	0.186	44.9	22.8	0.757	2.48	0.137	0.203	59.9	89.9
6	0.192	4.88	5.21	0.205	36.9	18.7	0.923	3.03	0.112	0.167	49.2	73.7
7	0.176	4.47	5.68	0.224	31.0	15.7	1.10	3.60	0.0941	0.140	41.3	62.0
8	0.160	4.06	6.25	0.246	25.6	13.0	1.33	4.36	0.0778	0.116	34.1	51.2
9	0.144	3.66	6.94	0.273	20.7	10.5	1.64	5.38	0.0630	0.0937	27.6	41.5
10	0.128	3.25	7.81	0.308	16.4	8.30	2.08	6.81	0.0498	0.0741	21.8	32.8
11	0.116	2.95	8.62	0.339	13.5	6.82	2.53	8.30	0.0409	0.0608	17.9	26.9
12	0.104	2.64	9.62	0.379	10.8	5.48	3.15	10.3	0.0329	0.0489	14.4	21.6
13	0.0920	2.34	10.9	0.428	8.46	4.29	4.02	13.2	0.0257	0.0383	11.3	16.9
14	0.0800	2.03	12.5	0.492	6.40	3.24	5.32	17.4	0.0194	0.0289	8.53	12.8
15	0.0720	1.83	13.9	0.547	5.18	2.63	6.56	21.5	0.0157	0.0234	6.91	10.4
16	0.0640	1.63	15.6	0.615	4.10	2.08	8.31	27.3	0.0124	0.0185	5.46	8.19
17	0.0560	1.42	17.9	0.703	3.14	1.59	10.9	35.6	0.00952	0.0142	4.18	6.27
18	0.0480	1.22	20.8	0.820	2.30	1.17	14.8	48.5	0.00700	0.0104	3.07	4.61
19	0.0400	1.02	25.0	0.984	1.60	0.811	21.3	69.8	0.00486	0.00723	2.13	3.20
20	0.0360	0.914	27.8	1.09	1.30	0.657	26.3	86.1	0.00394	0.00586	1.73	2.59
21	0.0320	0.813	31.3	1.23	1.02	0.519	33.2	109	0.00311	0.00463	1.37	2.05
22	0.0280	0.711	35.7	1.41	0.784	0.397	43.4	142	0.00238	0.00354	1.05	1.57